

Exploring DNA destabilization induced by the thymine dimer lesion using base
modifying probes and thermodynamic techniques

By
Amy Rumora

A thesis submitted to the Department of Biochemistry of Mount Holyoke College

Biochemistry Department
Mount Holyoke College
South Hadley, MA
May 2007

This thesis was completed
under the direction of
Dr. Megan Núñez
for twenty-four credits.

<u>Section:</u>	<u>Page number:</u>
Title	1
Research credits	2
Acknowledgments	3
Abstract	5
Chapter 1: Introduction	7
1.1 DNA structure and cellular context	7
1.2 DNA-damage and repair	11
1.3 The thymine dimer lesion	13
1.4 Chemical probe base modification	18
1.5 Thermodynamic experiments	22
1.6 Summary of expected results	24
Chapter 2: Methods	25
2.1 Oligonucleotide synthesis and purification	25
2.2 Cycloreversal characterization of the thymine dimer lesion	28
2.3 Labeling the DNA with radioactive isotope $\gamma^{32}\text{P}$	30
2.4 DNA concentration, annealing single-stranded DNA, and preparation of stock reaction mixtures	34
2.5 The small base modifying chemical reactions	36
2.6 Determination of DNA extinction coefficients	40
2.7 Thermodynamic techniques- van't Hoff analysis	42
2.8 Thermodynamic techniques: Differential Scanning Calorimetry	45
Chapter 3: Results	46
3.1 Characterization of single-strand DNA oligonucleotide	46
3.2 Determination of DNA extinction coefficients	51
3.3 Dimethyl Sulfate (DMS) base modifying reaction	54
3.4 Potassium Permanganate (KMnO_4) base modifying reaction	59
3.5 DMS and KMnO_4 base modifying reactions on AMM2	63
3.6 Diethylpyrocarbonate (DEPC) base modifying reactions	71
3.7 van't Hoff analysis	73
3.8 van't Hoff analysis in small chemical probe buffer	78
3.9 First derivative graphs	80
3.10 van't Hoff analysis of duplex containing the thymine dimer lesion	84
3.11 Differential Scanning Calorimetry	93
Chapter 4: Discussion	95
4.1 Characterization and purification of oligonucleotides	95
4.2 Accessibility to small chemical probes	96
4.3 Thermodynamic experiments	100
4.4 Chemical probe and thermodynamic experiments relate to previous studies	103

4.5 Considering kinetic base modification in addition to thermodynamic and structural studies will provide a better understanding of destabilization	104
4.6 Future Studies	106
References	108

ACKNOWLEDGEMENTS

I would like to thank my research mentor and thesis adviser for all her guidance and help during my thesis research. Thank you for all your help!

I would also like to thank Anne Malhowski for teaching and helping me when starting out on this research project!

Thank you to the Nunez Lab including Anne Malhowski, Catherine Volle, Amber Rosenberg, Aleksandra Mihailovic, Jackie Wade, Stephanie Azan, and Sara Barnes! You have been such amazing friends. Some of my fondest memories of Mount Holyoke will include late nights in lab, ice cream trips, Tim the glassblower, Dane Cook humor, Stephen Kellog, and the scary Aragorn cardboard cutout!

Thank you Sara Barnes for helping out with the long hours of HPLC purifying the oligonucleotides and listening to the pump clicking away all day long!

I would like to thank the chemistry and biochemistry departments for helping me to grow and learn through out my four years at Mount Holyoke College. Specifically, thank you to Lilian Hsu, for being such a wonderful academic adviser and professor! Also, thank you for the use of the phosphorimager and scintillation counter! Darren Hamilton, thank you for allowing me to use your UV-light box to synthesize the thymine dimer lesion. Thank you Wei Chen letting me borrow your cart and liquid nitrogen frequently! Thank you Eric Girard for helping out with dry ice. Lastly, I would like to thank

Sean Decatur for helping me to understand the intricacies of spectroscopy and calorimetry in Chem 315. Also, thank you for letting me use your lyophilizer.

Additionally, I would like to thank Elizabeth Jamieson from Smith College for allowing us to use her temperature controlled UV-Vis spectrophotometer when starting the thermodynamic experiments.

Lastly, I would like to thank my Grandpa and Grandma. Thank you Grandpa for showing me the magic in science all through my life. I hope that someday I can be as knowledgeable about scientific research as you are! Grandma, thank you for all your support and love!

I would like to thank my Mom, Dad, Matt, and Hanna for always listening and trying to understand my research when I talk about it. Thank you for being my support system during these four years of my life! You are the most amazing family anyone could hope for!

ABSTRACT

DNA frequently forms mutations due to endogenous or environmental conditions. During the Base Excision Repair pathway (BER), an enzyme removes damaged bases from DNA with a series of enzymatic steps. The thymine dimer lesion is formed from the cycloaddition of two same-strand, neighboring thymines. A kink in the duplex DNA occurs because the thymine dimer lesion cannot form hydrogen bonds with complementary adenines. Despite the extensive research done on the thymine dimer mutation and its repair mechanism, little is known about the way in which the specific BER enzyme locates the DNA lesion in order to carry out the BER pathway. It is possible that the thymine dimer lesion causes thermodynamic and kinetic destabilization to the DNA duplex.

In order to study DNA destabilization caused by the thymine dimer, DNA containing the dimer was purified and labeled with the radioactive isotope, $\gamma^{32}\text{P}$. The DNA was reacted with DNA base modifying chemical probes, Dimethyl Sulfate (DMS), Potassium Permanganate (KMnO_4), and Diethyl pyrocarbonate (DEPC). Following the base modification, the sugar phosphate backbone of the DNA was cleaved using piperidine. The fragments were observed using electrophoretic techniques. Data from this method has revealed significant reactivity of the bases around the thymine dimer. This suggests that the thymine dimer lesion kinetically destabilizes surrounding bases in duplex DNA.

A standard method for measuring destabilization induced by a DNA lesion involves thermodynamic techniques and optical measurements. A temperature-controlled UV-vis spectrophotometer was used to observe differences in the shape of the sigmoidal melting curves and thermodynamic parameters. Differential Scanning Calorimetry (DSC) was used to determine and confirm values obtained through spectrophotometry. The thermal melting of the B-form duplex strand contrasts with an enthalpically and thermally destabilizing thymine dimer duplex.

CHAPTER 1: INTRODUCTION

Deoxyribonucleic acid (DNA) encodes genetic information that instructs processes that sustain life. It is imperative that DNA remains error-free in order to maintain normal life. DNA mutations may result in disease or even fatality. To prevent mutations, repair pathways cut out the mutation and restore DNA to normalcy. This study focuses on the thymine dimer lesion and the thermodynamic and kinetic destabilization it induces in duplex DNA.

1.1 DNA Structure and Cellular Context

Deoxyribonucleic acid (DNA) is a polymer of nucleotides. Each nucleotide contains a single nitrogenous base, a deoxyribose sugar group, and a phosphate group. Purine bases, adenine and guanine, are composed of fused heterocyclic, five- and six-membered rings. Thymine and Cytosine are pyrimidine nitrogenous bases and are composed of a single six-membered ring. Bases are attached to the sugar group through a glycosidic bond. The phosphate group forms phosphodiester bonds with the C3' and C5' of the sugar groups creating the sugar-phosphate backbone of the DNA (Figure 1.1).

When single stranded DNA and its complimentary strand come together to form Watson-Crick base pairs, they form a 3' to 5' antiparallel double helix. Complimentary single-strand DNA molecules come together under the influence of hydrophobic interactions and stacking interactions formed from base pi-orbitals. The double helix is reinforced by hydrogen bonds. Hydrogen bonds

form between the hydrogen of an amino group on one nitrogenous base and the ring nitrogen or carbonyl oxygen of another. Guanine forms three bonds with cytosine so the base pair is stronger than the two hydrogen bonds that adenine forms with thymine (Figure 1.1 and 1.2). Therefore, a higher GC content will cause the two strands to have a stronger interaction while a higher TA content will cause two strands to have a less strong interaction (Breslauer *et al.*, 1986).

DNA is packed into chromosomes inside the eukaryotic cell nucleus. DNA encodes the genetic information expressing specific genes that instruct the synthesis of functional proteins during transcription and translation. When genetic mutations occur, the DNA replication process copies the mutation and DNA polymerases transcribe the mutation into templates. Mutations within an organism's genetic code may lead to disease. In order to maintain the correct genetic sequence, repair mechanisms allow for the removal and repair of genetic mutations.

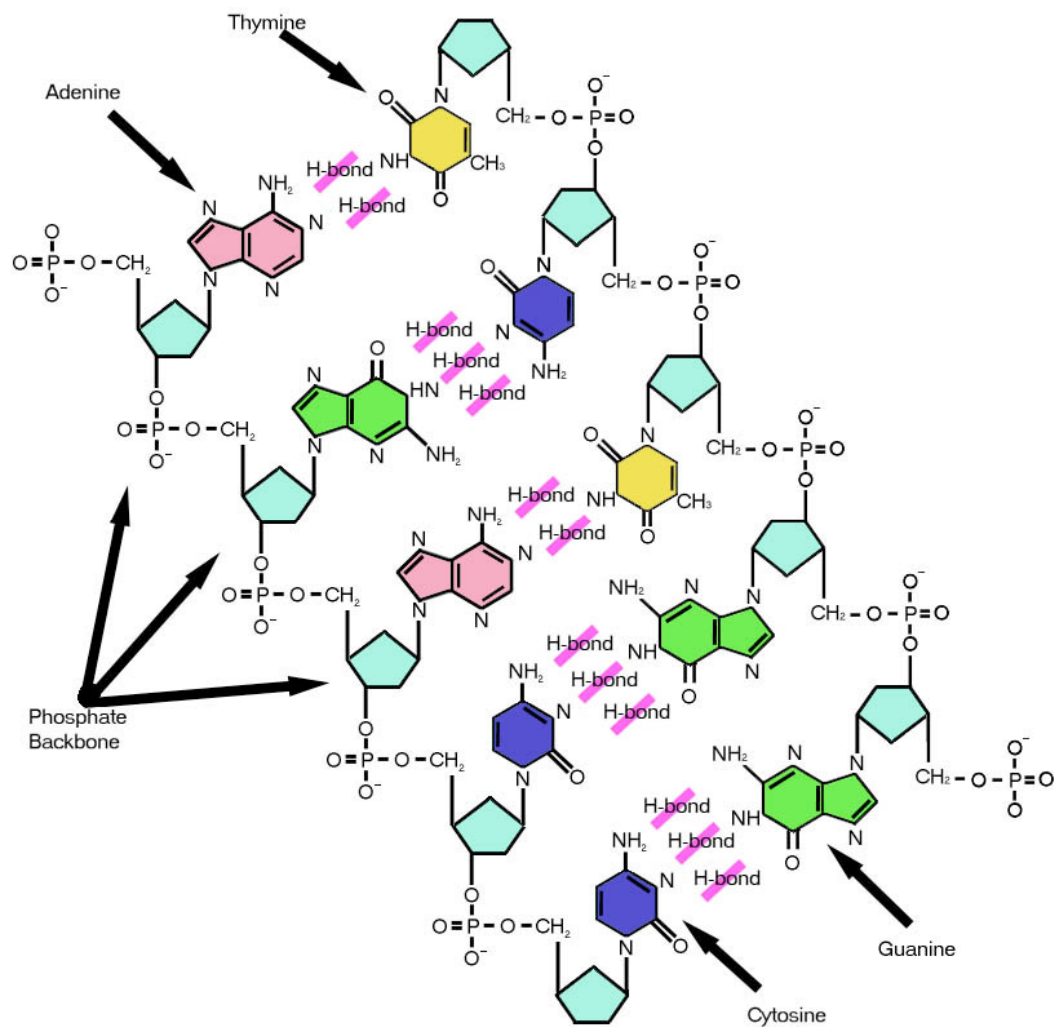


Figure 1.1- The structure of DNA. The polymer of nucleotides is linked together by interactions between phosphate groups and deoxyribose sugar groups. In the center of the helix, purine bases interact with pyrimidine bases through hydrogen bonding. (Figure adapted from http://www.wordiq.com/knowledge/images/7/76/DNA_labels.jpg)

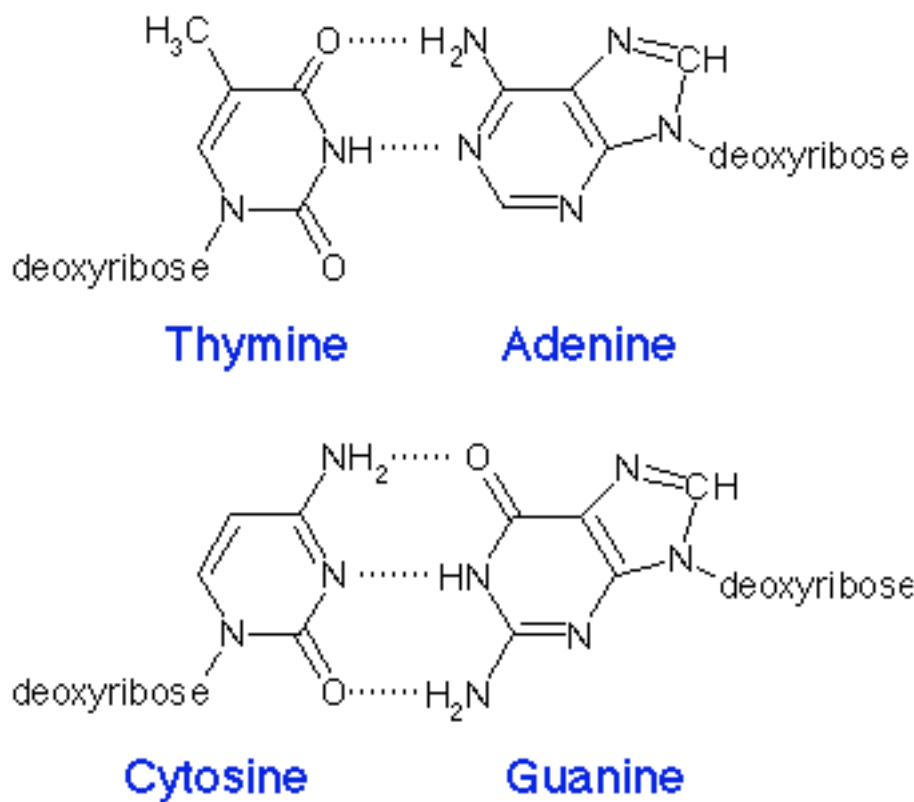


Figure 1.2- Watson–crick base pairing holds the complementary strands of DNA together. Three hydrogen bonds form between cytosine and guanine while only two hydrogen bonds form between thymine and adenine. (Figure adapted from <http://138.192.68.68/bio/Courses/biochem2/GeneIntro/DNAandRNAIntro.html>)

1.2 DNA-damage and repair

DNA mutations occur frequently and are caused by both environmental and endogenous causes. Endogenous mutations occur within cells due to reactive oxygen species. Such mutations also arise naturally in processes such as replication and mutation repair. Exogenous or environmental causes of mutations are external to the cell and include factors such as chemical changes, radiation, or UV-light. Without a repair system, these mutations would lead to transcriptional and translational errors and ultimately disease or fatality. However, two repair pathways eliminate these errors: Base Excision Repair (BER) and Nucleotide Excision Repair (NER).

Endogenous mutations form due to oxygen radicals that are byproducts of mitochondrial cellular respiration. A well-researched mutation of this type is called 8-oxoguanine. This mutation occurs when guanine bases are exposed to reactive metabolites that oxidize guanine at the 8-position. This oxidation of the guanine base results in a mutation that selectively binds to Adenine over Cytosine (Bruner *et al.*, 2000). Another type of endogenous mutation is formed due to transitions from cytosine to thymine at CpG sites. The oxidation of 5-methylcytosine is one example of this transition (Marnett *et al.*, 2001). In addition, high temperature causes cleavage of purine bases. Depurination, the cleavage of glycosidic bonds between the nitrogenous base and nucleotide, occurs naturally but increases at high temperatures decreases at low pH (Friedberg *et al.*, 1995)

Exogenous mutations arise from external conditions. The most well known exogenous mutation is the thymine dimer lesion. This lesion results from UV-light radiation of two thymine bases and the formation of a *cis, syn*-cyclobutane thymine dimer. The thymine dimer fails to form hydrogen bonds and perturbs duplex DNA. It is the lesion of focus in this study.

In Nucleotide Excision Repair, enzymes excise whole fragments of mutated DNA strands in order to remove bulky lesions. A DNA lesion is recognized by the NER enzyme, the duplex DNA is separated in the area around the lesion, and an excision of single-strand DNA containing the lesion removes the damaged DNA. In the final stages of NER, the gap is filled in by DNA synthesis and the remaining nick is ligated (Nelson and Cox, 2004).

Base Excision Repair is responsible for removing small base mutations. The BER pathway involves a BER enzyme excising out single base mutations in three steps. First, the BER enzyme specific to that pathway removes the mutated base. This creates an AP site. Second, an AP endonuclease creates a 3'-OH terminus next to the AP site. Third, a DNA polymerase then lengthens the 3'-OH terminus and excises the AP site. We focus on the BER of an environmentally caused mutation, the thymine dimer (Nelson and Cox, 2004).

1.3 The thymine dimer lesion:

When a DNA strand, containing neighboring thymine bases, is exposed to UV-light at a wavelength of 200-300 nm, it forms the *cis, syn*-cyclobutane thymine dimer. Structurally, UV-light causes two covalent bonds to form between the 5, 6 double bonded carbons. This formation of covalent bonds conjoins the two pyrimidines forming a dimer through cycloaddition (Figure 1.3).

The structural details pertaining to *cis, syn*-cyclobutane thymine dimers are depicted (Figure 1.4). The two thymines form covalent bonds so that the heterocyclic rings are on the same side of the cyclobutane ring forming a *cis* conformation. The hydrogen and $-\text{CH}_3$ groups stick out in front of the cyclobutane ring. In the *trans, syn* thymine dimer, these two groups stick out behind the cyclobutane ring. In the *cis, syn*-cyclobutane thymine dimer, the thymines are arranged in the *syn* position meaning they are positioned in the same directions (Figure 1.4).

The thymine dimer is a well-researched DNA lesion. It can cause melanoma, a malignant form of skin cancer. Husain *et al.* explored the structural distortions caused by the thymine dimer lesion. Using two-dimensional gel electrophoresis and quantitative electron microscopy, they found that the thymine dimer causes a kink in the DNA (Figure 1.5). The cycloaddition of the two thymines disables them from base pairing within the DNA. This disturbs the overall B-form DNA causing it to bend about 30° (Husain *et al.*, 1988).

Another investigation by Park *et al.* analyzed the unbound crystal structure of B-form DNA containing a *cis-syn* thymine dimer. The structure shows an overall helical bending of about 30° and unwinding of about 9°. Local perturbations are also prominent in the damaged DNA. These effects include a broad minor and major groove and lack of base pairing (Park *et al.*, 2002).

Despite the extensive research done on the thymine dimer mutation and its repair mechanism, little is known about the way in which the specific repair enzyme locates the DNA lesion in order to carry out the repair pathway. It is possible that the thymine dimer lesion causes destabilization to the DNA strand in which it is located.

An analysis by Anne Malhowski revealed significant reactivity of the bases around the thymine dimer using Dimethyl Sulfate (DMS) and Potassium Permanganate (KMnO₄) reactions. She analyzed the effect of these reagents on a control duplex (lacking the thymine dimer lesion) and an experimental duplex (containing the thymine dimer lesion). The control was the strand AMM1*-AMM2 (where * means radioactive and the strand being analyzed) and did not contain the thymine dimer lesion. The experimental strand was AMMTT*-AMM2 and contained the thymine dimer lesion. Her data supported the idea that the dimer causes thermodynamic and kinetic destabilization, which would draw the BER enzyme to the area of the lesion. We will test the same hypothesis by confirming Anne's findings with DMS and KMnO₄ reactions and run DMS and KMnO₄ reactions on the two complimentary strands of DNA, AMM1-AMM2*

and AMMTT-AMM2*. In addition, we will perform experiments using the base modifying chemical probe diethylpyrocarbonate (DEPC).

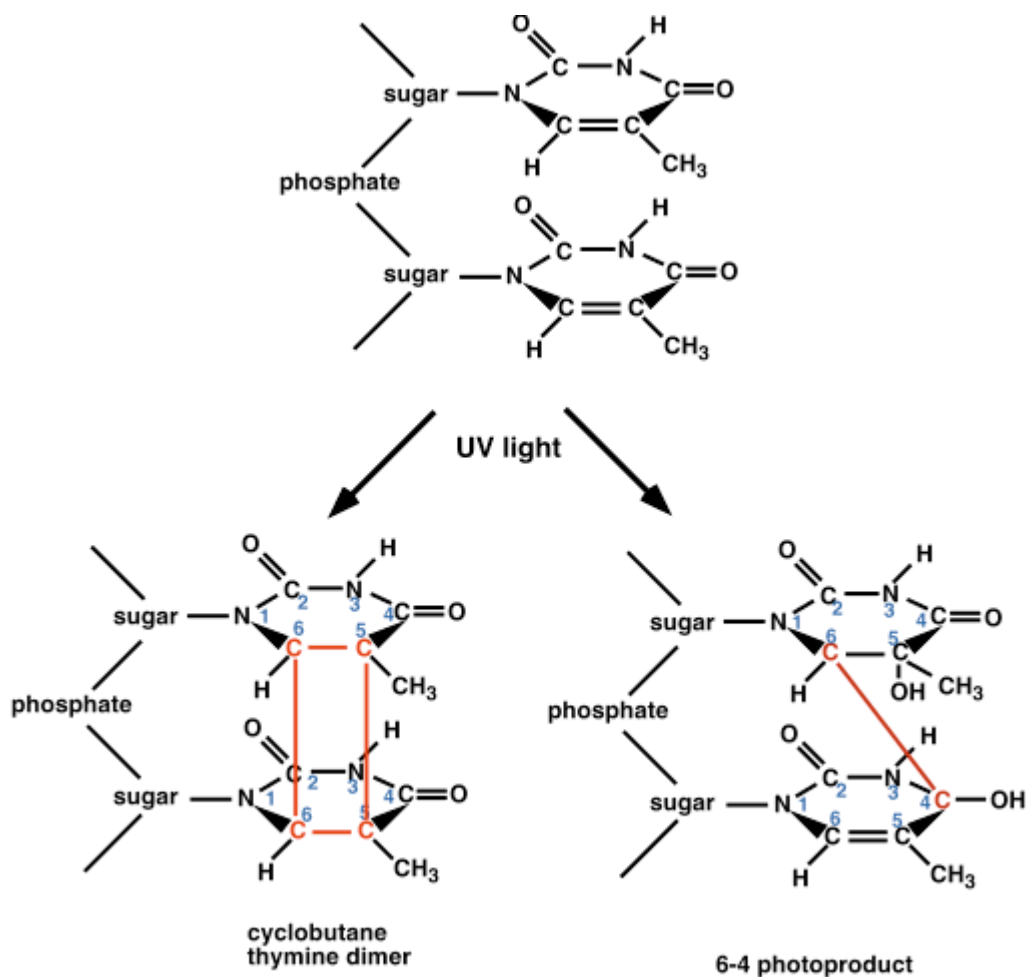


Figure 1.3- Thymine dimers are formed by a cycloaddition of two adjacent thymines irradiated by UV light 200-300 nm. There is a formation of two bonds at C5 and C6. This forms the cyclobutane thymine dimer. A 6-4 photoproduct is a by-product of the irradiation.

(Figure from <http://www.public.asu.edu/~iangould/reallife/thymine/thymine.html>)

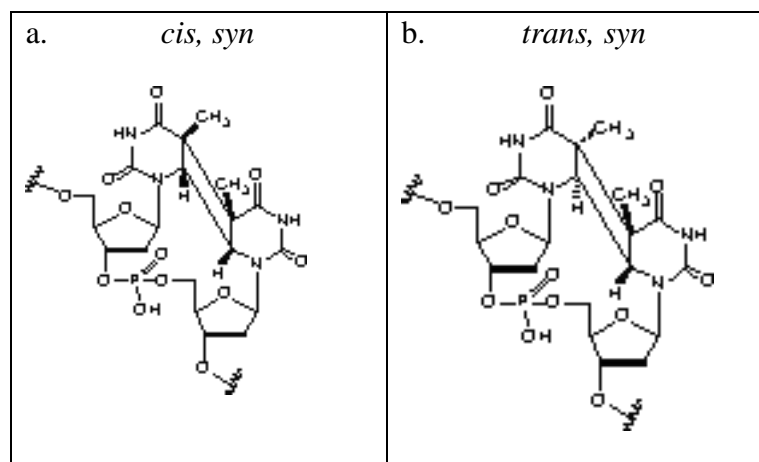


Figure 1.4- Cyclobutane thymine dimers form many different conformations under irradiation of UV-light. (Panel a) The *cis, syn*-cyclobutane conformation forms two covalent bonds so that the heterocyclic rings are on the same side of the cyclobutane ring forming a *cis* conformation. The hydrogen and -CH₃ group stick out in front of the cyclobutane ring. (Panel b) In the *trans, syn* thymine dimer a hydrogen and -CH₃ group stick out behind the cyclobutane ring. (Figures adapted from Glen Research)

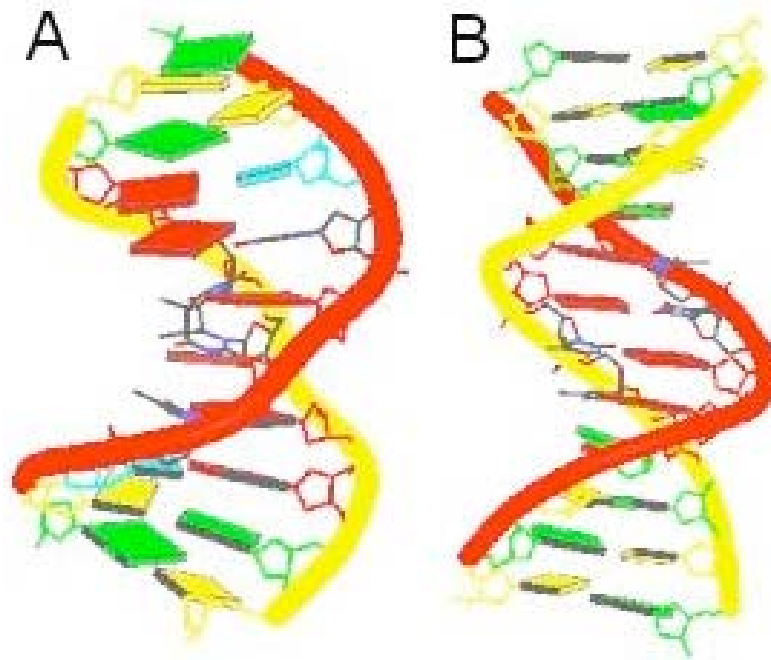


Figure 1.5- A structural comparison of modified and unmodified DNA (Panel A) DNA with a thymine dimer lesion. The dimer kinks the helical structure bending it by about 30° . (Panel B) B-form DNA without a lesion does not have a kink. The clear helical structure is visible. (Figure adapted from Park *et al.*, 2002 and Brown *et al.*, 1986)

1.4 Chemical probe base modification:

After labeling the DNA with the radioactive probe, $\gamma^{32}\text{P}$, we reacted it with a reagent that is a DNA base modifier. DMS as a reagent for base modification reacts with N7 of guanine bases and 10% piperidine cleaves the sugar phosphate backbone leaving fragments of DNA (Figure 1.6). KMnO_4 reacts with the C5 and C6 in thymine bases and 10% piperidine leaves different sized DNA fragments (Figure 1.7). DEPC reacts with the N7 of purine bases (Figure 1.8)

I hypothesize that the reactivity of the base will increase with time and temperature. It is also likely that the reactivity of surrounding bases and those within the dimer will be different in KMnO_4 reactions. The reason this is likely is that the areas for modification may not be accessible to the reagent due to the thymine dimer. Also, if the dimer causes increased destabilization of the bases around it, the bases in the strand containing the dimer lesion will show more reactivity than those in the control strand.

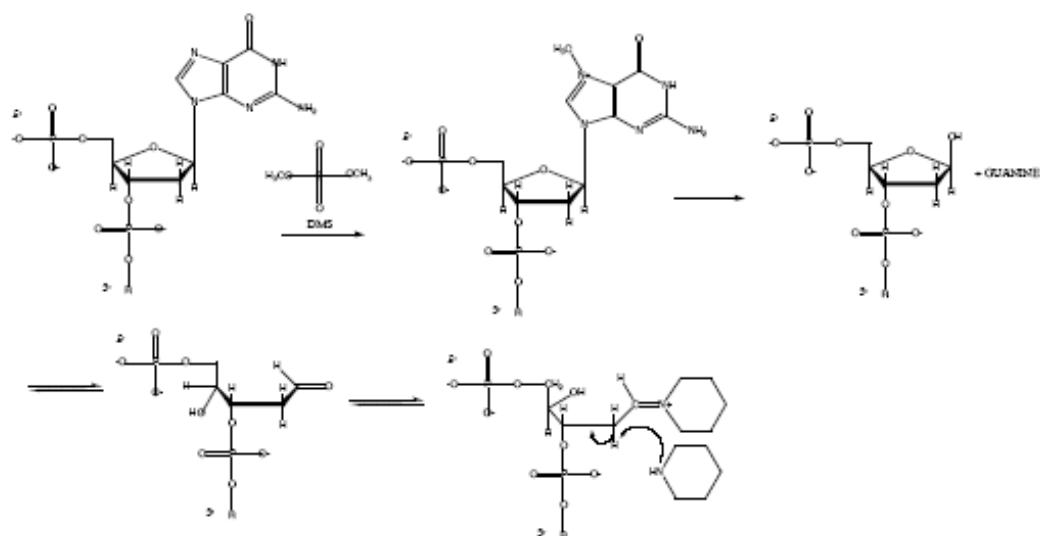


Figure 1.6- In the DMS reaction Dimethyl Sulfate reacts with N7 in guanines. The 10% piperidine then cleaves the sugar phosphate backbone (Nunez, 2004).

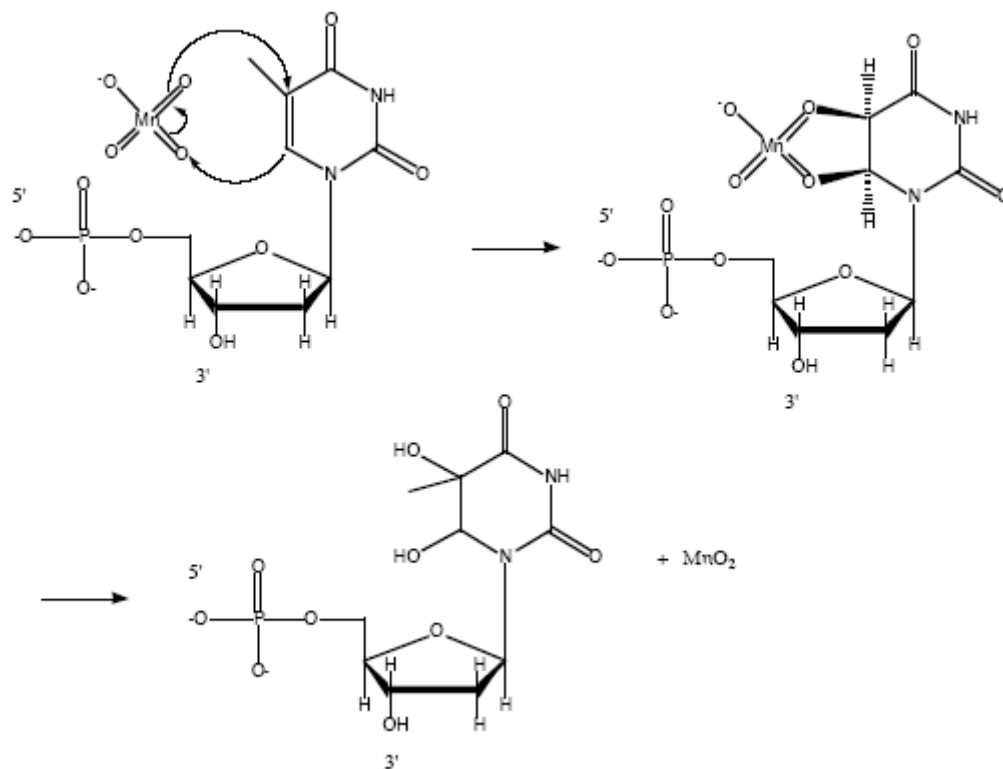


Figure 1.7- In the Potassium Permanganate reaction, KMnO_4 reacts with C5 and C6 of thymine. 10% piperidine then cleaves the sugar phosphate backbone (Figure adapted from Bruice, 1999).

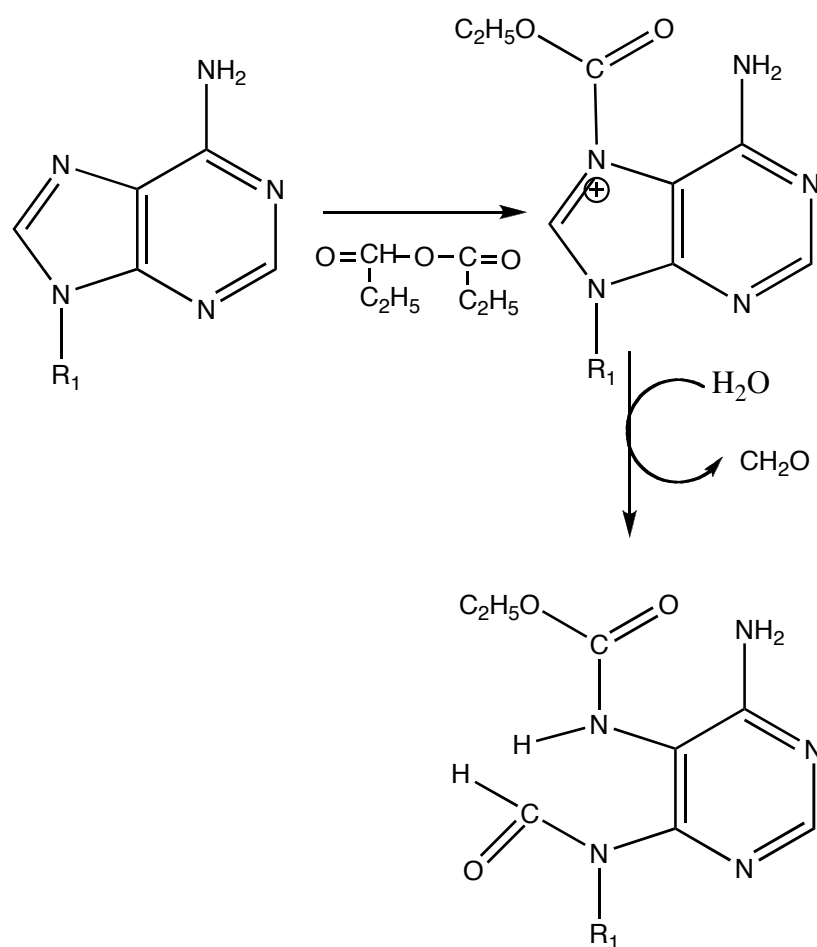


Figure 1.8- In the Diethylpyrocarbonate reaction, modification occurs at the N7 of purine bases. 10% piperidine then cleaves the sugar phosphate backbone (Figure adapted from Ehresmann *et al.* 1987).

1.5 Thermodynamic experiments:

The thymine dimer lesion perturbs duplex DNA because it fails to form hydrogen bonds with complementary adenine bases. This causes a kink in the DNA. The lesion may induce thermodynamic destabilization of duplex DNA. A standard method for examining thermodynamic destabilization induced by a lesion employs optical measurements such as spectroscopy and calorimetry.

Previous studies indicate that DNA mutations induce significant changes in thermodynamic parameters. An exocyclic base adduct called 3,N⁴-deoxyethenocytosine (ϵ C) causes a decrease in duplex stability despite sequence context changes. This study showed enthalpic reductions of 4.6 ± 2.5 kcal/mole for the ϵ C-T model (Gelfand *et al.*, 1998).

In another study, an anticancer drug called cisplatin is used to bind and crosslink DNA to form an adduct. Thermal stability is lowered by about 9 °C and enthalpic stability is lowered by 15 kcal/mol when the adduct is present in duplex DNA. On the other hand, the cisplatin adduct tends to stabilize the DNA entropically by about 35 cal/K**mol* (Poklar *et al.*, 1996).

Lastly, a study investigating the propane-dG lesion and the 8-oxoguanine lesion found that significant changes in the T_m occurred. However, this does not indicate a correlation with free energy. They find that changes in entropy and enthalpy compensate for one another so that the overall free energy difference is minimized (Plum *et al.*, 1994).

We will perform similar thermodynamic experiments on a duplex containing the thymine dimer lesion and compare resulting thermodynamic values to those of a duplex without the lesion. UV-vis spectroscopy is used to measure the absorbance of DNA as it becomes unannealed with increasing temperature. Differential Scanning Calorimetry is used to measure changes in heat capacity in the samples as temperature increases.

1.6 Summary of expected results

It is likely that the DMS chemical probe experiments will show similar results for both strands of DNA. I hypothesize that the reactivity of the base will increase with time and temperature. This seems likely because the areas of reactivity for these reactions are accessible to the reagent in both strands. It is also likely that the reactivity of surrounding bases and those within the dimer will be different for the KMnO_4 reactions. The reason this is likely is that the areas for modification may not be accessible to the reagent due to the thymine dimer. Also, if the dimer causes increased reactivity of the bases around it, the bases in the strand containing the dimer lesion will show more reactivity than those in the control strand. Lastly, the DEPC reactions will likely lead to increased reactivity in the strand containing the thymine dimer lesion but only at purine bases.

Thermodynamic experiments will most likely show a trend of reduced enthalpy and increased entropy in the presence of the thymine dimer lesion in comparison to the unmodified duplex. In addition, it is likely the melting temperature will shift to a lower temperature when the duplex contains the thymine dimer lesion. This is a fairly consistent trend across most experiments exploring thermodynamic destabilization of various DNA lesions.

CHAPTER 2- METHODS

2.1 Oligonucleotide synthesis and purification:

The oligonucleotides used in this experiment were obtained from Integrated DNA Technologies. They were 19-mer DNA strands from a 1 μ mol synthesis. Two different sequences were used. The first sequence was AMM1 and contained two neighboring thymines, which would form a thymine dimer under the influence of UV- light. AMM2 was composed of the complementary sequence (Figure 2.1).

The DNA arrived in lyophilized form and was suspended in 500 μ L of 1X TE. The solution of 1X TE was a dilution of 10X TE that was composed of 100 mM Tris (pH=7.4) and 10 mM EDTA (pH=8.0). Each sample was then filtered through micro-filter tubes. Reversed-phase HPLC was used to purify each sample of 200 μ L. A C-18 reversed-phase column was used with a flow rate of 4 μ L/min. The gradient conditions used for the reverse-phase HPLC are shown in table 2.1. AMM1 eluted from the column at about 12 minutes and AMM2 eluted at about 19 minutes. The purified DNA was collected at the time of elution. They were then freeze-dried by placing them in liquid-nitrogen (-196 °C). A lyophilizer was then used to dry them completely.

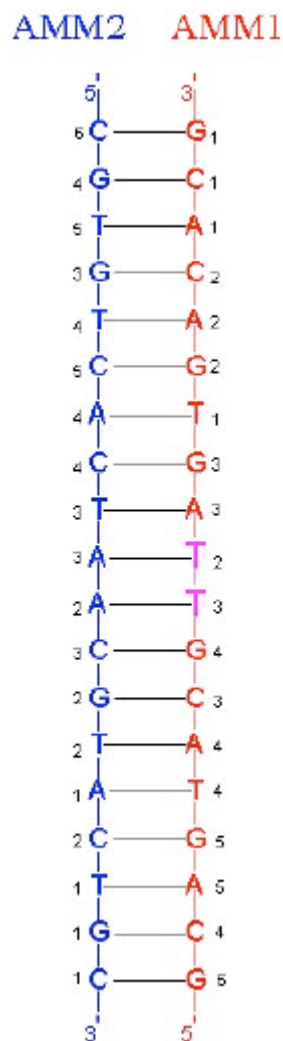


Figure 2.1. AMM1 is the 19-mer strand of DNA shown in red. Under irradiation, the two neighboring thymines 2 and 3 form a thymine dimer to make the strand, AMM1TT. AMM2 is the 19-mer strand of DNA shown in blue (Malhowski, 2005). Numbers along the sides of the sequences indicate the base number as shown on gel electrophoresis pictures.

The AMM1TT strand was then created from AMM1. The 2.4 mg of AMM1 DNA was resuspended in 1 mL of 0.1 M sodium phosphate buffer with a pH of 7.4. Half of the solution was then mixed with 3.66 μ L 25 mM acetophenone. The solution was then syringed into the round bottom area of the specialized vacuum-cuvette complex. A freeze-pump-thaw process was used to rid the sample of oxygen. The sample was frozen in liquid nitrogen, placed under a vacuum for 5 seconds, then nitrogen gas was applied to the sample and the sample was then allowed to thaw and melt back to liquid state. This process was repeated 4 additional times. The remaining solution was then moved to the cuvette in the glassware and placed in a UV light box and irradiated at 300nm for about 3 hours.

The dimer was then purified on a C-18 column with HPLC. An injection of 100 μ l was run through the HPLC under a program with the gradients (Table 2.2). The AMM1TT DNA was fractionated from the left over AMM1 and other byproducts. The purified AMM1TT DNA was collected and frozen in liquid nitrogen and then placed on a lyophilizer until dry. Each sample of AMM1TT DNA was resuspended in 100 μ L 1X TE solution.

2.2 Cycloreversal characterization of the thymine dimer lesion:

A cycloreversal method was used to confirm the presence of the thymine dimer lesion. A solution containing 350 μL of AMM1TT and 1 mL of 0.1 M sodium phosphate buffer were mixed in a quartz cuvette and irradiated under UV-light between 200-300 nm for one hour. Following the cycloreversal procedure, HPLC was used to confirm the reversal back to separate thymines. Three injections including pure AMM1, pure AMM1TT, and the cycloreversal sample were run and assessed for reversal of the thymine dimers to single thymines.

Table 2.1- Gradient conditions for purifying AMM1 and AMM2

Time (mins)	% acetonitrile	% 25 mM ammonium acetate
0	5	95
5	5	95
25	10	90
30	5	95

Table 2.2- HPLC gradients for purifying AMM1TT from AMM1 and byproducts.

Time(mins)	% acetophenone	% 25 mM ammonium acetate
0	2	98
7	3	97
20	8	92
25	10	90
30	50	50
35	50	50
40	5	95
45	5	95

2.3 Labeling the DNA with radioactive isotope $\gamma^{32}\text{P}$:

In order to probe each base of the DNA strand, the DNA was labeled with the radioactive isotope, $\gamma^{32}\text{P}$. This was attached to the 5'-end of the DNA. The stock reaction mixture included 8 μM ssDNA, 5 μL PNK enzyme buffer, and dH_2O . The $[\gamma^{32}\text{P}]\text{ATP}$ label was thawed at 37 °C for about 45 minutes and then proportionately added to each reaction mixture. An amount of 1 μL PNK enzyme was added to each mixture. They were then incubated at 37 °C for 1.5 hours.

Ethanol precipitation allowed for the removal of salt in each solution. Amounts of 570 μL 100% ethanol, 75 μL 7.5 mM NH_4OAc and 100 μL dH_2O were added to each sample. Incubation at -78 °C precipitated the DNA for 0.5 hrs and centrifugation at 12,000 rpm (4 °C) for 12 minutes allowed the DNA to form a pellet at the bottom of the eppendorf tube. The pellet was then rinsed with 80% cold ethanol and centrifuged for 2 minutes under the same conditions. The samples were then partially suspended in 20 μL 1X TE buffer and dried in the speedvac. A piperidine treatment then exposed the cleaved areas of the DNA. In the treatment 10% piperidine solution was added to each sample and incubated at 90 °C for 30 minutes. Each sample was then diluted with 20 μL dH_2O and placed in the speedvac until it was completely dry.

An 18 % polyacrylamide gel solution was polymerized for purification of the DNA. The solution was composed of 101 mL SequaGel concentrate, 25 mL SequaGel diluent, 14 mL SequaGel Buffer, 600 μL 10 % ammonium persulfate,

and 30 μ L TEMED. The gel was allowed to warm up with an electrical current of 40 watts for 1 hour (Sambrook, 2001).

Each ssDNA sample had 20 μ L of running dye added to it and was vortexed vigorously. The samples were heated at 90 °C for 5-10 minutes. The Prep gel was run at 40 watts for about 3.25 hours.

In complete darkness, the gel was placed on top of a piece of film and allowed to develop for 5 minutes. It was then placed in developer for 3 minutes and then fixer for 3 minutes. It was then placed in the water. The bands containing the radioactive ssDNA were cut out of the gel and placed in eppendorf tubes. An amount of 1 ml of 1X TE was added to each tube and they were crushed with a spatula. They were then vortexed and incubated at 37 °C for 1 hour, vortexing every 15 minutes. This was repeated and each sample and allowed to sit in the refrigerator overnight. The supernatant liquid and gel bits were then filtered through micro-filter tubes in a centrifuge for 12 minutes at 25 °C at 12,000 rpm.

The last part of radioactive labeling was running the ssDNA through Nensorb 20 cartridge columns. The volumes of liquids that were run through the columns are given in table 2.3. In the last step, the solution containing the 50% MeOH/ 50% dH₂O was sucked through the column until the column was completely dry. This allowed the DNA to elute from the column. The samples were then dried overnight on the speedvac. The samples were run on the scintillation counter in order to obtain a radioactivity count on each sample.

Table 2.3- Volumes of liquids used for sample purification by Nensorb 20 cartridge columns.

Amount of fluids added to column	Type of liquids
1 volume	Methanol (MeOH)
2 volumes	1X TE
All	Samples
3 volumes	1X TE
2 volumes	dH ₂ O
2 mL	50% MeOH/ 50% dH ₂ O

2.4 DNA concentration, annealing single-stranded DNA, and preparation of stock reaction mixtures

The concentration for each ssDNA was obtained in order to run reactions. The UV-visible spectrophotometer was set at an absorbance of 260 nm. The absorbencies were then multiplied by their dilution factor. Beer's Law was then used to calculate the concentration for each sample. The following concentrations are given in table 2.4.

The ssDNA was labeled and purified. In order to run reactions the single stranded DNA was annealed together. The first set of dsDNA that was tested was AMM1*-AMM2 and AMM1TT*-AMM2 and was prepared for each reaction. So stock reaction mixtures were formed with the two types of 8 μ M ssDNA, the selected buffer, and dH₂O.

The DMS stock reaction mixtures were prepared in DMS buffer. The KMnO₄ and DEPC stock reaction mixtures were prepared in 0.1 M Sodium Cacodylate (pH=6.5) and 0.125 M EDTA. The stock reaction mixtures were added to a tube of dried ssDNA. They were vortexed vigorously and allowed to anneal on a 90 °C heat block which was turned off for about 1 hour and 30 minutes or until the temperature went down to 30 °C. The solutions were then split into 20 μ L volumes into the eppendorf tubes.

Table 2.4- Concentrations for ssDNA AMM1, AMM2, and AMM1TT.

ssDNA	Concentration
AMM1	360 μM
AMM2	411 μM
AMM1TT	84 μM

2.5 The small base modifying chemical reactions:

Ethanol precipitation then aided in pelleting the DNA. Immediately after being removed from the dry ice, the samples were centrifuged for 12 minutes at 12,000 rpm at 4 °C in order to pellet the DNA. The supernatant was then removed without disturbing the pellet. Each pellet was then rinsed with 100 µL of 80% cold ethanol and centrifuged for 2 minutes at 12,000 rpm at 4 °C. The supernatant was again removed and 20 µL of 1X TE was added to each sample. They were then dried in the speedvac.

Each sample was then piperidine treated in order to expose the damaged sites of the DNA. To each sample, 100 µL of 10% piperidine was added and allowed to incubate at 90 °C for 30 minutes. The samples were then allowed to cool for about 10-15 minutes. The samples were then placed in the speedvac until dryness. Following, 20 µL of dH₂O was added to each sample and allowed to speedvac until dryness.

In the DMS reaction, the stock solution was split among 20 tubes, with 20 µL stock reaction solution per tube. This reaction was run at 3 different temperatures, 0 °C, 25 °C, and 37 °C each for 1, 2, and 5 minutes. The separate reaction tubes were preincubated at their designated temperatures for 5 minutes. 5 µL of 2.5% DMS solution (5 µL DMS and 195 µL dH₂O) was added to each sample and allowed to react at the specific temperature for the specific amount of time. The reaction was stopped after the correct amount of time by adding 20 µL DMS stop solution and mixing well for 2 minutes. Next, 120 µL of 100% ethanol

was added to each sample and the DNA was precipitated on dry ice for 15 minutes. The samples were then ethanol precipitated and piperidine treated as described previously.

In the KMnO_4 reaction, the stock solution was split among 20 tubes, with 60 μL stock reaction solution per tube. This reaction was run at 3 different temperatures, 0 °C, 25 °C, and 37 °C each for 2, 4, and 6 minutes. The separate reaction tubes were pre-incubated at their designated temperatures for 5 minutes. 1.5 μL of the 62.5 mM KMnO_4 solution was added to each sample and allowed to react at the specific temperature for the specific amount of time. The reaction was stopped after the correct amount of time by adding 300 μL DMS stop solution and mixing well for 2 minutes. Next 750 μL of 100% ethanol was added to each sample and the DNA was precipitated on dry ice for 15 minutes. The samples were then ethanol precipitated and piperidine treated as described previously.

In the DEPC reaction, the stock solution was split among 20 tubes, with 20 μL of stock reaction solution per tube. The reaction was performed at two different temperatures room temperature and 37 °C each for 0.25, 0.5, 1, 1.5, 2, and 3 hours. The separate reaction tubes were preincubated at their designated temperatures for 5 minutes. Separate reaction gels were run for the addition of 2, 3, and 5 μL of the 10% DEPC solution to each sample and allowed to react at the designated temperature and time. The reaction was stopped after the correct amount of time by adding 20 μL of DMS stop solution and mixing well for 2 minutes. 150 μL of 100% ethanol was then added to each sample and the DNA

was precipitated on dry ice for 1 hour. The samples were then ethanol precipitated and piperidine treated as described previously.

A 20% polyacrylamide gel solution was polymerized for separation of the bases and observation of the reactions (Sambrook, 2001). The gel was allowed to warm up with an electrical current of 45 watts for 1 hour. The reaction samples were run on the scintillation counter in order to obtain a radioactivity count. For every 10,000 cpm, 1 μ L of running dye was added. The samples were then vortexed vigorously and incubated at 90 °C for 5-10 minutes. The samples were then injected into the gel and the gel was allowed to run for about 3 hours and 15 minutes.

The gel was then removed from the plates with the aid of a scrap piece of film to remove it from the gel plate. It was then saran wrapped and placed on the phosphorimager developer plate for at least 5 hours. The phosphorimager then read the developer plate and created a picture of the gel and location of the differently cleaved strands of DNA. With the background set at none, the percentage that one band stood for out of the whole lane represented the final percentage for that base. These were then graphed in order to observe any differences in reactivity.

Finally, the DMS and KMnO_4 reactions were repeated for the strands AMM1-AMM2* and AMMTT-AMM2*. In this case the complimentary strands were labeled with $\gamma^{32}\text{P}$. The DMS and KMnO_4 reactions were completed using the same methods.

2.6 Determination of DNA extinction coefficients:

Using the first method, we calculated extinction coefficients by finding the sum of extinction coefficients of all individual bases. In other words, each base has a molar extinction coefficient (A=15000, G=12300, C=6700, and T=7400) that can be multiplied by the number of that base within the strand. Once all four bases have been accounted for, they are summed to a final extinction coefficient, which is vital in calculating concentrations of oligonucleotide in samples.

A second method called “nearest neighbors”, was used to determine the extinction coefficient of a DNA oligonucleotide strands using dinucleotide pairs. Each pair has a characteristic extinction coefficient, which was accounted for in sets of two bases. The sum of base extinction coefficients was then subtracted from this value to obtain a revised extinction coefficient. In addition, different sources had different dinucleotide extinction coefficients. In order to obtain the most accurate extinction coefficient we performed calculations for each different set of dinucleotide extinction coefficients (Devor *et al.*, 2005 and Cantor *et al.*, 1980).

Snake Venom Phosphodiesterase (SVP) analysis was used to cleave the sugar-phosphate backbone of the oligonucleotides. The SVP was resuspended in 1000 μL of 100 mM sodium phosphate buffer. Using two matched quartz cuvettes, the mixtures of solutions were prepared separately. In the first cuvette, 10 μL of 15 mM MgCl_2 , 200 μL of Tris buffer (pH=9), 706.4 μL of water, and 41.8 μL of SVP were mixed. The absorbance of this solution was measured in the

UV-visible spectrophotometer as the blank. In a second matching quartz cuvette, 10 μL of 15mM MgCl_2 , 200 μL of Tris buffer (pH=9), 706.4 μL of water, and 41.8 μL of AMM1 were measured in the UV-visible spectrophotometer as A0. To this cuvette, 41.8 μL of SVP were added with a Hamilton syringe for accuracy. An initial absorbance, A1, was taken immediately after the addition of SVP. Additional absorbance points (A2...A3...A4...A5...etc.) were taken each minute after the addition of SVP. After several samples, the absorbance leveled off and remained within a short range of the maximum absorbance value. An average of these absorbance measurements was used to calculate the new extinction coefficient. This average represents the final absorbance of oligonucleotide and SVP.

In the SVP analysis calculations, the SVP absorbance was subtracted from the averaged absorbance of SVP plus oligonucleotide. The absorbance of the oligonucleotide before the SVP was divided by the absorbance of oligonucleotide after the SVP was added. This number was then multiplied by our original extinction coefficient to obtain a revised extinction coefficient for each oligonucleotide.

2.7 Thermodynamic techniques- van't Hoff analysis

The single strand DNA strands were annealed to form stock reaction mixtures containing 0.1 M phosphate buffer, water, and either AMM1-AMM2 duplex or AMM1TT-AMM2 duplex as previously described. The AMM1TT DNA was synthesized by phosphoramidite chemistry. In preparation for thermal experiments, the samples were degassed in a Microcal DSC degasser for 15-20 minutes at 25 °C until no air bubbles were visible. Small stir bars and a medium stir speed were used to ensure minimal air bubbles.

An Ultraviolet Visible Spectrophotometer was set for the following conditions. The UV/vis spectrophotometer was zeroed with 0.1 M phosphate buffer at a wavelength of 260 nm. The sample was placed in a cuvette with a lid and parafilm to prevent evaporation. The sample was heated from 20 °C to 70 °C at 260 nm. The melting curve was observed and the melting temperature T_m was determined using the first derivative of the sigmoidal melting curve.

Cuvettes with varying pathlengths were used to change the concentration of the DNA being melted. The cuvette sizes and corresponding DNA concentrations are given in table 2.5. The different sized cuvettes were accommodated into the UV/vis Spectrophotometer cuvette holder with a small metal insert, which aided in conducting heat to the cuvette. A van't Hoff plot was determined using the melting temperature (T_m) results and the concentration of the sample from the varying melting of the various concentration of DNA.

The van't Hoff analysis assumes that duplex annealing and unannealing is a two-state process lacking thermodynamic contributions from intermediate states. The slope of the line in the van't Hoff plot and the intercept were plugged into the van't Hoff equation (Equation 1). This equation was derived from the Gibbs free energy equation and the van't Hoff law. It is commonly used when studying the thermodynamic impact of DNA lesions. The resulting values were entropy, enthalpy, and free energy.

$$\frac{1}{T_m} = \frac{R}{\Delta H_{vH}} \ln C_{tot} + \frac{\Delta S_{vH} - 1.39R}{\Delta H_{vH}}$$

Equation 1. The van't Hoff equation was derived from the Gibbs free energy equation. Thermodynamic parameters are calculated this equation and the slope and y-intercept from the van't Hoff plot.

Table 2.5- Cuvette pathlength and corresponding DNA concentration.

Cuvette pathlength (cm)	DNA concentration (μM)
1	0.79
1	2
0.5	4.2
0.2	11
0.1	21

2.8 Thermodynamic techniques: Differential Scanning Calorimetry (DSC):

Preparation for the Differential Scanning Calorimetry experiments also required the annealing and degassing of AMM1-AMM2 and AMM1TT-AMM2 duplexes as described previously. The DSC was set up to go through 10 upscans going from 10 °C to 90 °C and 10 downscans going from 90 °C to 10 °C. Each scan began with a 15 minute prescan and end with a 15 minute postscan. 0.1 M phosphate buffer was injected into both the sample and reference cells in the DSC. After several buffer scans were taken, the 0.1 M phosphate buffer was removed from the sample cell and replaced with the sample. After the 20 scans, the scan graphs were imported and normalized to obtain information about Gibbs free energy (ΔG), enthalpy (ΔH), the heat capacity (ΔC_p), the melting temperature (T_m), and entropy (ΔS). Using the origin program, the buffer scan was subtracted from the sample scan, the plot was normalized, and a baseline was selected. The plot was fixed under a 2-state model and origin calculated the exact T_m , enthalpy, and heat capacity contributions. The origin program can also be used to plot the Gibbs free energy plot.

CHAPTER 3- RESULTS

3.1 Characterization of single-strand DNA oligonucleotides

The study of the thymine dimer lesion in duplex DNA requires synthesis, purification, and characterization. The synthesis of the thymine dimer lesion occurred near the center of the single-strand DNA where two neighboring, same-strand thymines were positioned. The centered arrangement of the thymine dimer allows bases located further down the DNA strand to sense the lesion's existence. High Performance Liquid Chromatography (HPLC) purification was used to isolate the thymine dimer lesion from other byproducts formed during the synthesis. Characterization of the thymine dimer containing oligonucleotide through cycloreversal and HPLC confirms that the mutation is a thymine dimer lesion and that it is in correct conformation.

Following the thymine dimer synthesis, several techniques allowed us to distinguish the thymine dimer strand from other byproducts of UV irradiation and the unmodified strand. The single-strand oligonucleotide containing the *cis,syn*-cyclobutane thymine dimer lesion was confirmed through cycloreversal of the thymine dimer. Unmodified and modified oligonucleotides were characterized by HPLC. The thymine dimer containing oligonucleotide was purified from acetophenone, byproducts, and unmodified oligonucleotides.

Cycloreversal of the thymine dimer lesion was used to confirm the presence of the thymine dimer lesion in the oligonucleotide. Exposure to UV-light causes a correctly synthesized thymine dimer to break covalent bonds

between the thymine bases. Using HPLC, a change in the ratio between AMM1 and AMM1TT before and after cycloreversal is visible. In figure 3.1 the intensity of the AMM1 peak increases while the intensity of the AMM1TT peak decreases. Therefore, the thymine dimer was correctly synthesized and is reversed to separate thymine bases with irradiation by UV-light of 300 nm.

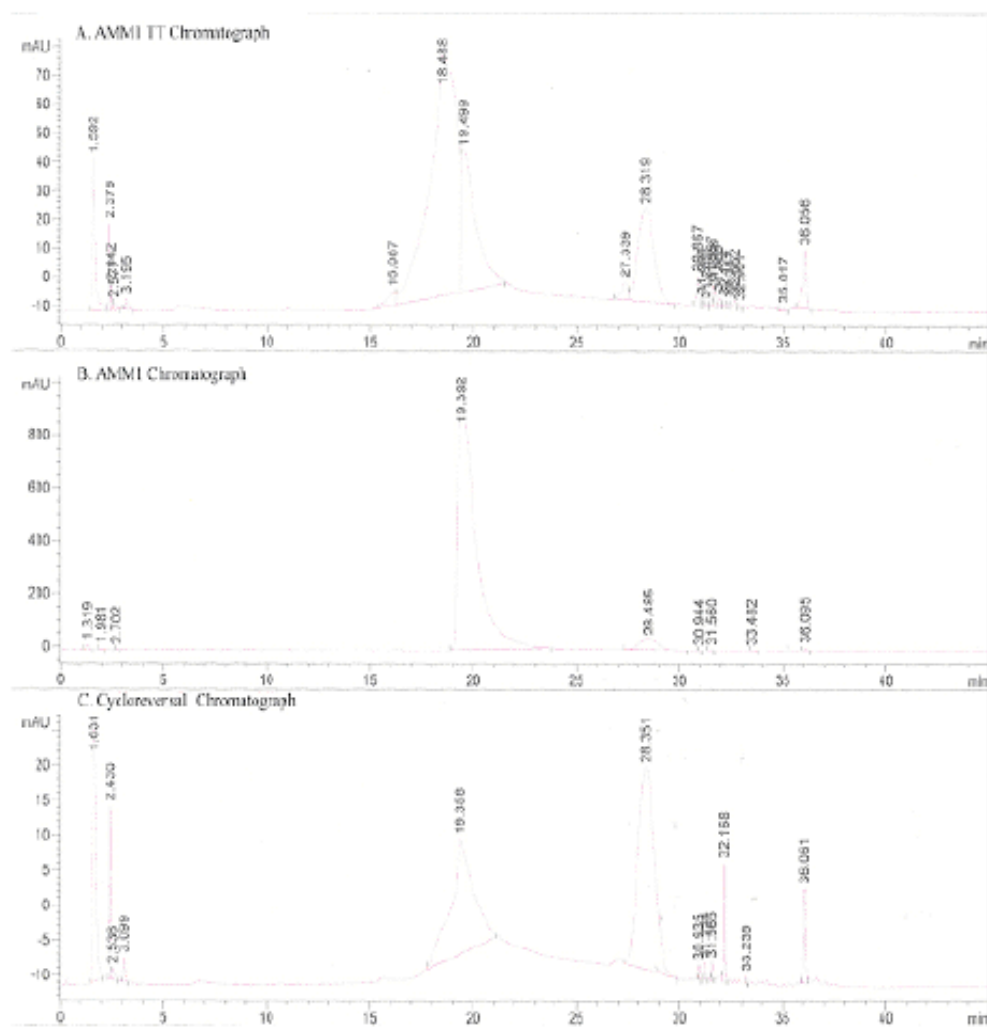


Figure 3.1 Cycloreversal graphs show successful cycloreversion of the thymine dimer lesion. (Panel A) One peak is visible where AMM1TT elutes at about 18.5 minutes. (Panel B) One peak is visible where AMM1 elutes at 19.3 minutes. (Panel C) A shift is visible in the cycloreversal sample shows an oligonucleotide that elutes at 19.3. This elution time is characteristic of AMM1.

HPLC was used to characterize and isolate specific products of the thymine dimer synthesis based on shape and elution time of each peak. The graph obtained from reverse-phase HPLC of the thymine dimer synthesis products is shown in figure 3.2. The AMM1TT peak elutes directly before the AMM1 peak at around 18.0 minutes and has a broad, plateau shape. The AMM1 peak elutes immediately after the AMM1TT strand at around 20.1 minutes. This sharp peak is much larger than the AMM1TT peak because the thymine dimer synthesis reaction does not proceed to completion and the AMM1TT yield is small in comparison to the unmodified AMM1 DNA. The point where the AMM1TT and AMM1 peaks meet contains both AMM1 and AMM1TT. Acetophenone elutes at 33.9 minutes in a tall, sharp peak and byproducts elute between 20-30 minutes in tiny peaks. The thymine dimer synthesis resulted in a very small yield. The base modifying probe experiments required very little DNA and the AMM1TT synthesized in lab was sufficient for completing those experiments.

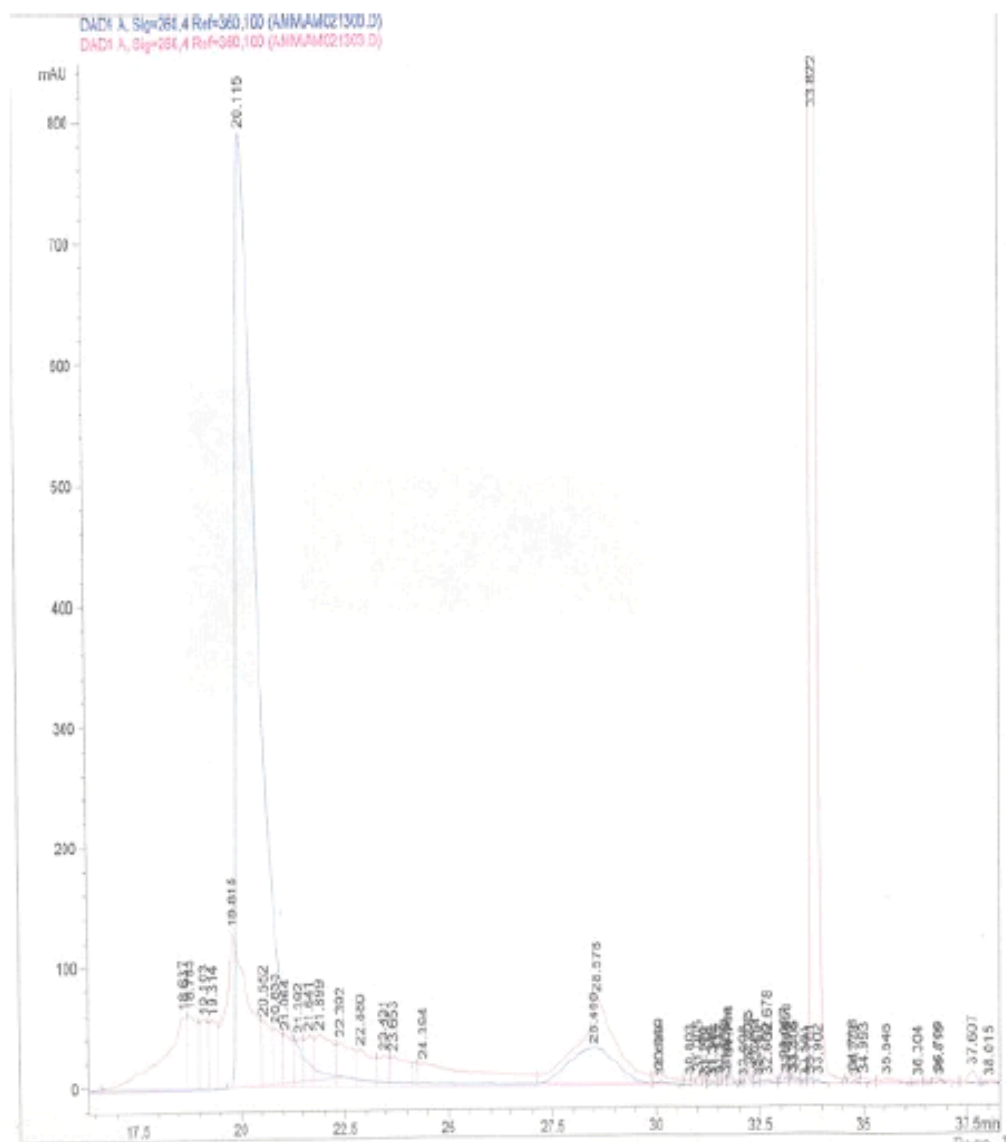


Figure 3.2. HPLC signal overlay of AMM1TT and AMM1. Shown in blue, AMM1 elutes in one tall peak around 20.1. AMM1TT elutes around 18.0 minutes in a broad peak immediately before AMM1.

3.2 Determination of DNA Extinction Coefficients:

When performing thermodynamic experiments, accurate concentrations of DNA are extremely important because concentration influences the thermodynamic measurements. We used several methods to determine extinction coefficients of the DNA including adding extinction coefficients base by base, the nearest neighbor method, and the Snake Venom Phosphodiesterase (SVP) analysis.

Using the first method, we calculated extinction coefficients by finding the sum of extinction coefficients of all individual bases. DNA concentration is calculated with about 10% accuracy using this method. Although this method is adequate for most applications, single strand DNA has a lower extinction coefficient than individual bases because base stacking quenches some of the absorbance in ultraviolet light. Thermodynamic measurements require a more accurate determination that takes base pair stacking into account.

A second method called “nearest neighbors,” was used to determine the extinction coefficient of a DNA strand using dinucleotide pairs. Each pair has a characteristic extinction coefficient. They were added up and the sum of extinction coefficients from mononucleotides was subtracted out.

The use of Snake Venom Phosphodiesterase (SVP) cleaves the sugar-phosphate backbone of DNA and causes an increase in signal intensity. SVP cleaves the DNA backbone into mononucleotides from the 3' end to 5' end of the DNA. The increase is measured after several minutes when the cleavage of the

DNA is completed. The increase is measured and used to calculate a revised extinction coefficient.

The calculated extinction coefficients are shown in table 3.1. They were calculated and compared. We chose to use the extinction coefficients obtained through the SVP analysis. These extinction coefficients were modified for accuracy by the SVP analysis but close to the extinction coefficients used in the base modification experiments. The extinction coefficients obtained through the SVP analysis tended to fall in the middle of the range of extinction coefficients calculated. We used extinction coefficient 190000 for calculating AMM1 and AMM1TT concentrations and extinction coefficient 175000 for calculating AMM2 concentrations.

Table 3.1 Extinction coefficients (EC) calculated for the sum of mononucleotide (ECs), the nearest neighbor's method, and the SVP analysis.

	AMM1	AMM2
Sum of mononucleotide extinction coefficients	205200	176500
Sum of new mononucleotide extinction coefficients	210400	195500
Nearest neighbor's	186600	176500
Nearest neighbor's (IDT)	186600	176500
SVP analysis	190000	175000
Final value	190000	175000

3.3 Dimethyl Sulfate (DMS) base modifying reaction:

Dimethyl Sulfate (DMS) is a small base modifying chemical probe that methylates the N7 of guanine bases, which is located in the major groove of the DNA. Base modification by DMS serves as a control experiment because guanine bases are accessible to DMS modification independent of the existence or absence of the thymine dimer lesion. We expected to see an equal amount of guanine base reactivity in both the modified and unmodified DNA. The modified and unmodified DNA was reacted with DMS at varying times and temperatures. All guanine bands showed distinct reactivity. Other than some over cleavage of bands, all darkened bands appeared to be of about the same intensity. This represents the guanines in duplex DNA that were reacted with DMS.

Under the influence of 2.5% DMS, methylation occurs at the N7 of Guanine bases. Both AMM1*-AMM2 and AMM1TT*-AMM2 showed darker bands representing different length segments ending with a guanine. At 0 °C, the bands for both AMM1*-AMM2 and AMM1TT*-AMM2 were light despite the increase in time increments. This represents minimal reactivity. At 25 °C, the darkness of the bands increased with time, representing an increase in reactivity for both strands. The same trend was visible at 37 °C with increasing time increments. Both DNA strands had similar results in terms of guanine reactivity (Figure 3.3). The graphs of the individual guanines showed overlapping reactivity (Figure 3.4). Each of the 5 affected guanines show the trends of the

AMM1*-AMM2 and AMM1TT*-AMM2 to be about the same. There was no extreme difference in reactivity.

Looking at the two new strands, AMM1-AMM2* and AMM1TT-AMM2*, we observe the way a thymine dimer lesion affects the base reactivity on the complimentary strand. Measuring reactivity of cross-strand thymines improves our understanding of the thymine dimers influence on the overall localized region of the duplex DNA. The results of the DMS and KMnO_4 reactions were similar to those obtained with the previous strands used.

The DMS reactions showed little difference in reactivity between the DNA strand containing the lesion and the DNA strand without the lesion. Only three guanines were visible on the gel. All had increasing reactivity with time and temperature. The gel shows little difference in reactivity of guanines with DMS (Figure 3.7). The graphs show a consistent overlap of reactivity of the two different strands (Figure 3.8 and 3.9).

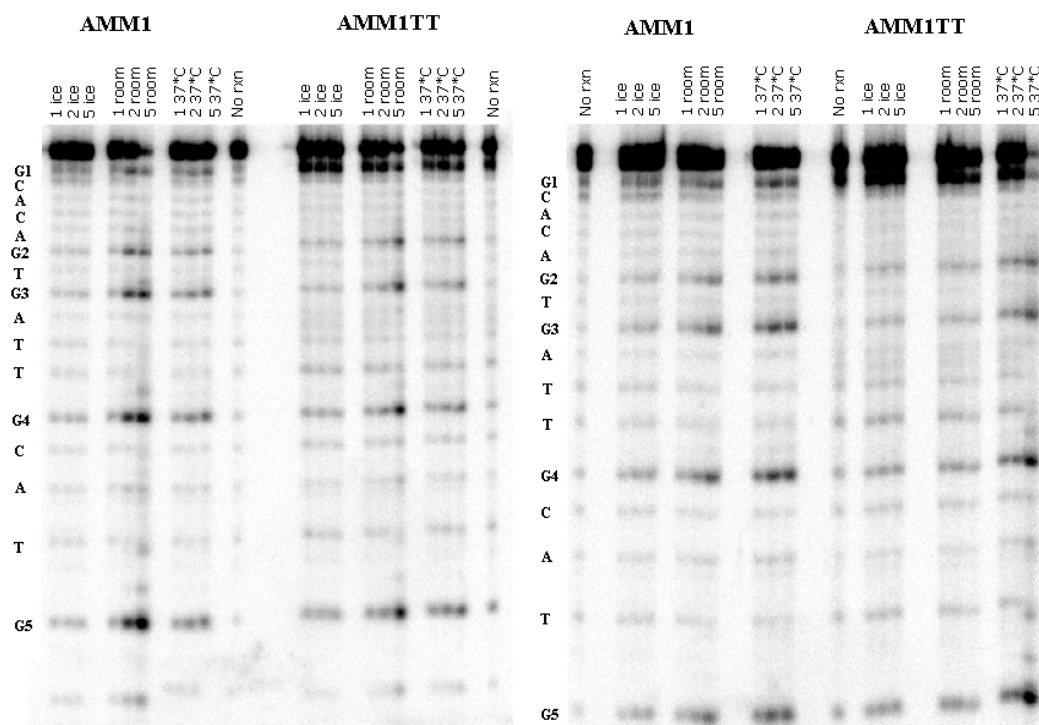
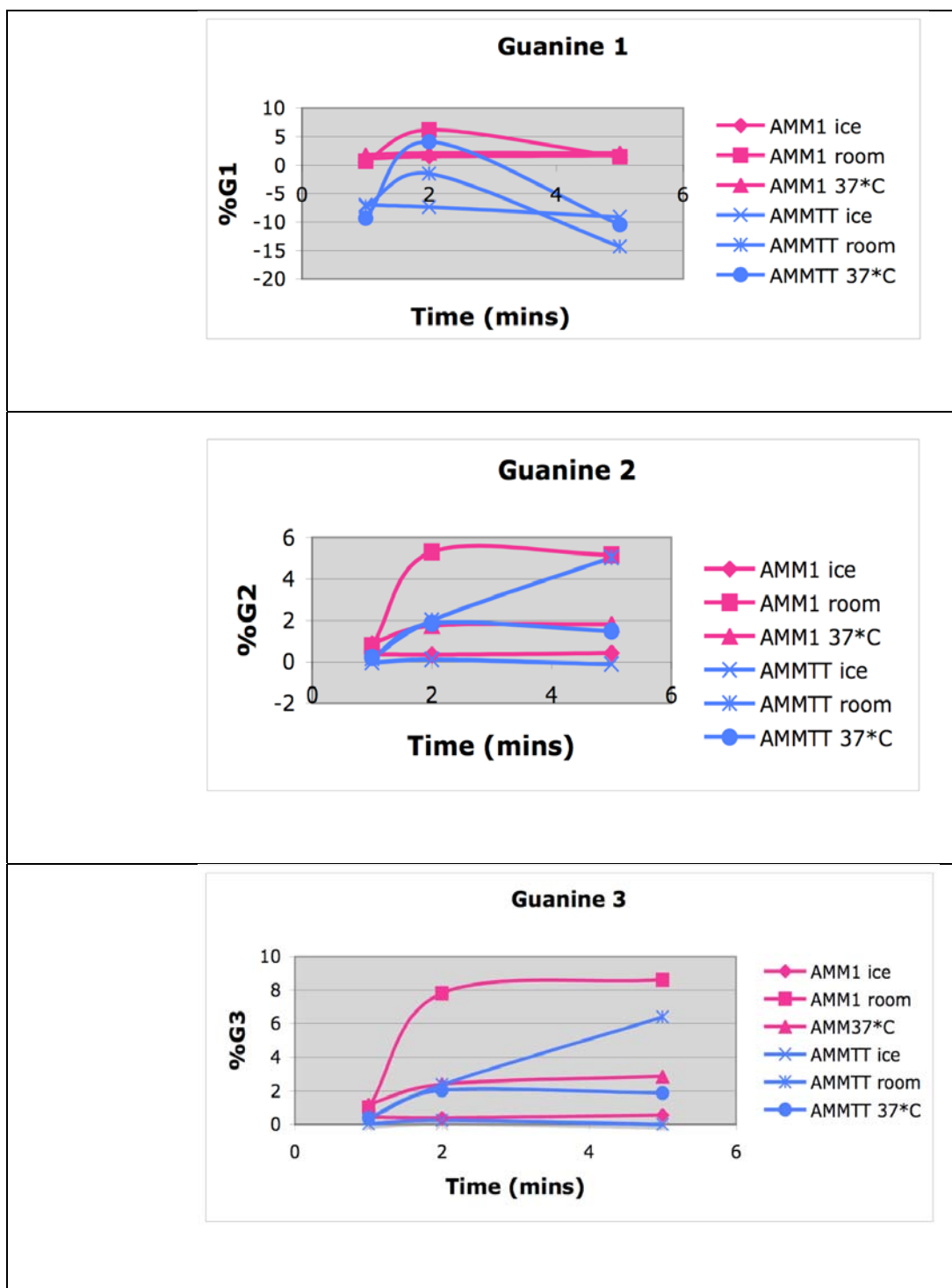


Figure 3.3. These two DMS reaction gels of strands AMM1*-AMM2 and AMM1TT*-AMM2 show similar trends of reactivity for both strands of DNA.



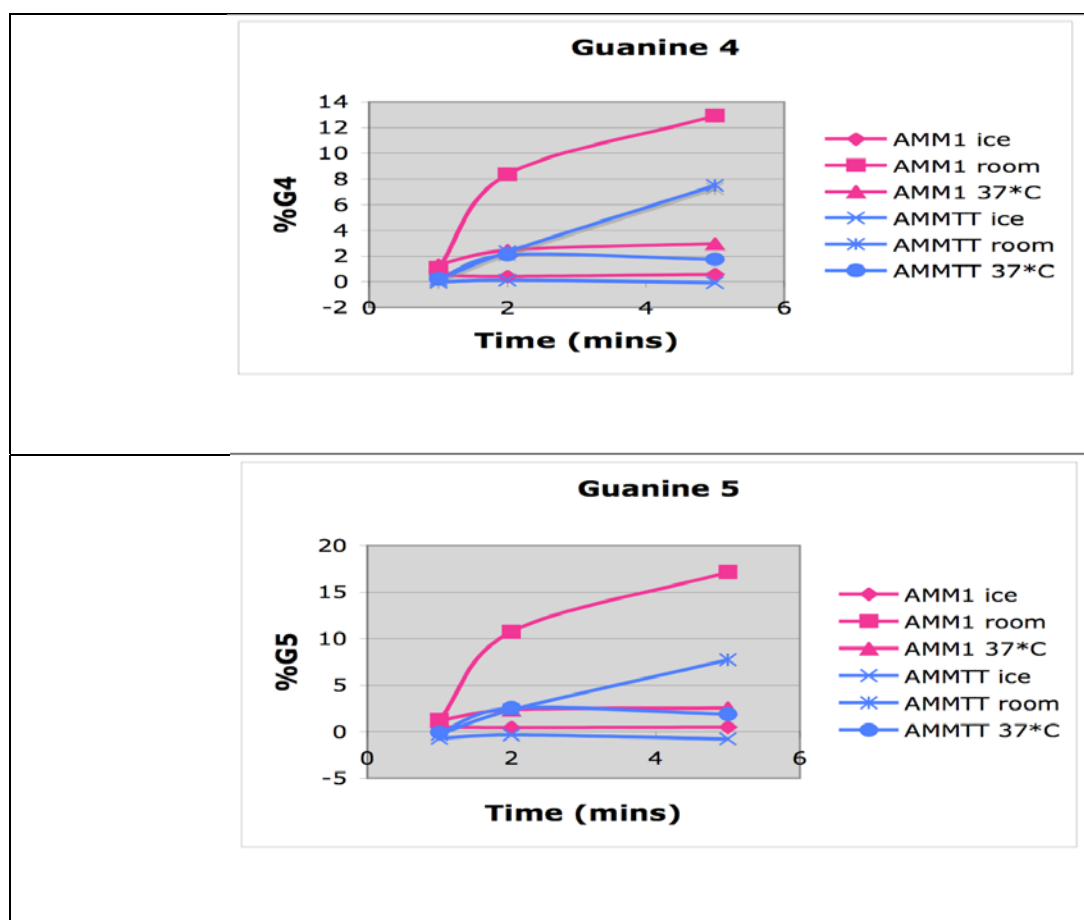


Figure 3.4. These graphs show the overlapping % reactivity from the two strands AMM1*-AMM2 and AMM1TT*-AMM2. There were 5 guanines that showed up on the gel. The information for these graphs was obtained from DMS gel A (Figure 3.3).

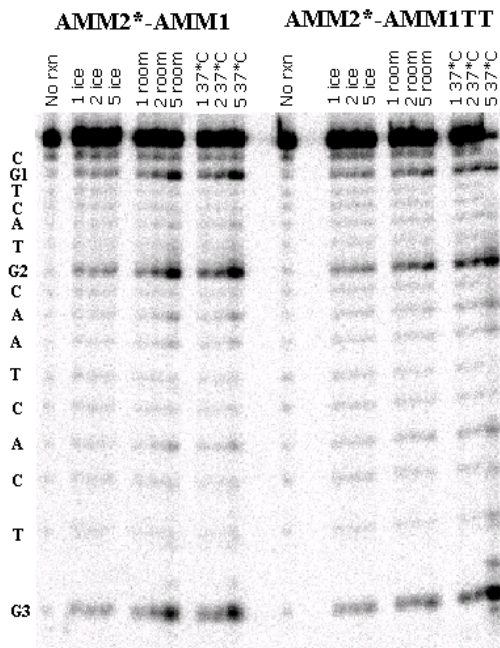


Figure 3.7. These DMS gels show fairly equal amounts of radioactivity between each guanine. The gels show three reacting guanines on strands AMM2*-AMM1 and AMM2*-AMM1TT.

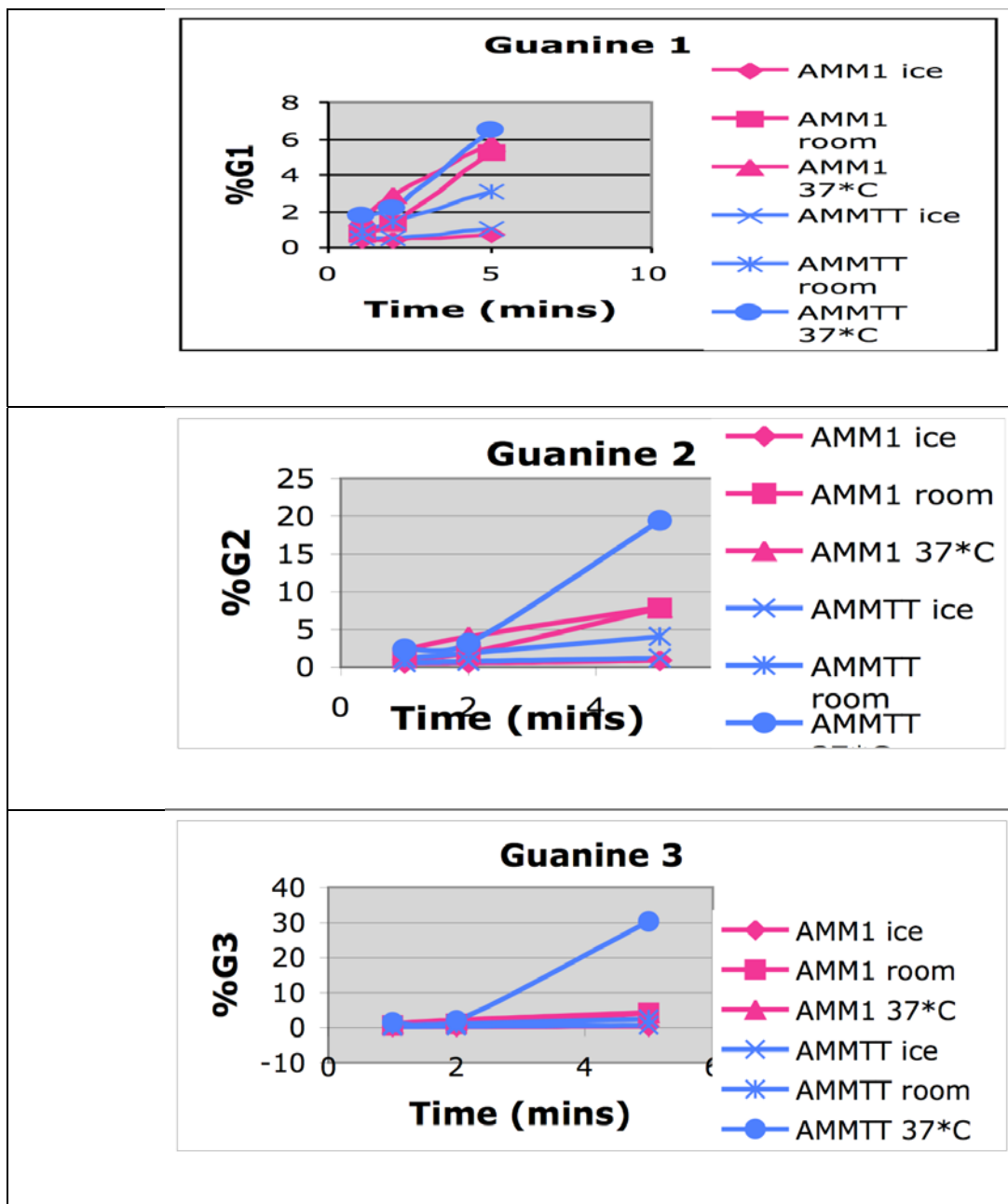


Figure 3.9. These graphs were obtained from information from DMS gel (figure 3.7) looking at AMM2*-AMM1 and AMM2*-AMM1TT. They show overlapping trends of reactivity.

3.4 Potassium Permanganate (KMnO₄) base modifying reaction:

Potassium Permanganate (KMnO₄) is a base modifying chemical probe that modifies the C5 and C6 of thymine bases. We use base modification by KMnO₄ to explore the effect of the thymine dimer lesion on bases around it because thymine bases should be more accessible to KMnO₄ in a destabilized strand of duplex DNA. The modified and unmodified DNA was reacted with KMnO₄ at varying times and temperatures. The thymine bases surrounding the B-form duplex DNA were less reactive than those surrounding the thymine dimer lesion.

The reaction of KMnO₄ with thymine bases generated a huge difference in modification and cleavage between the strands AMM1*-AMM2 and AMM1TT*-AMM2. Four thymines were affected by the KMnO₄ reaction and were shown on the gel. The reactivity increased with time and temperature in most cases. There are two different thymine environments that must be observed; those thymine bases adjacent (1 and 4) to the thymine dimer lesion, and (2 and 3) those within it (Figure 3.5). When looking at the graphs, it is obvious that the thymines adjacent to the dimer were more reactive to the KMnO₄ base modifier than the adjacent thymines on the control strand lacking the thymine dimer lesion (Figure 3.6). On the other hand, the thymine bases within the lesion show little to no reactivity. The control strand does not contain a lesion; instead it has two neighboring thymines next to each other. These thymines show a huge amount of reactivity.

The KMnO_4 gel of AMM2* shows reactivity compatible with the information from the gels of AMM1* and AMM1TT* (Figure 3.10). The graphs show high-level reactivity of cross-strand, adjacent thymines to the dimer (Figure 3.11). The strand without the dimer shows little reactivity of these thymines. Again, increasing temperature and time play a large part in the amount of reactivity visible.

It must be noted that the graphs reported in this results section are representative of one gel, which is specified with the graphs. The graphs and data are not compiled because it is useful to observe the bands on the gel to understand trends. Each gel is slightly different making it difficult to compile the data. In addition, over cleavage of a single reaction throws off trends when depicted in a compiled graph.

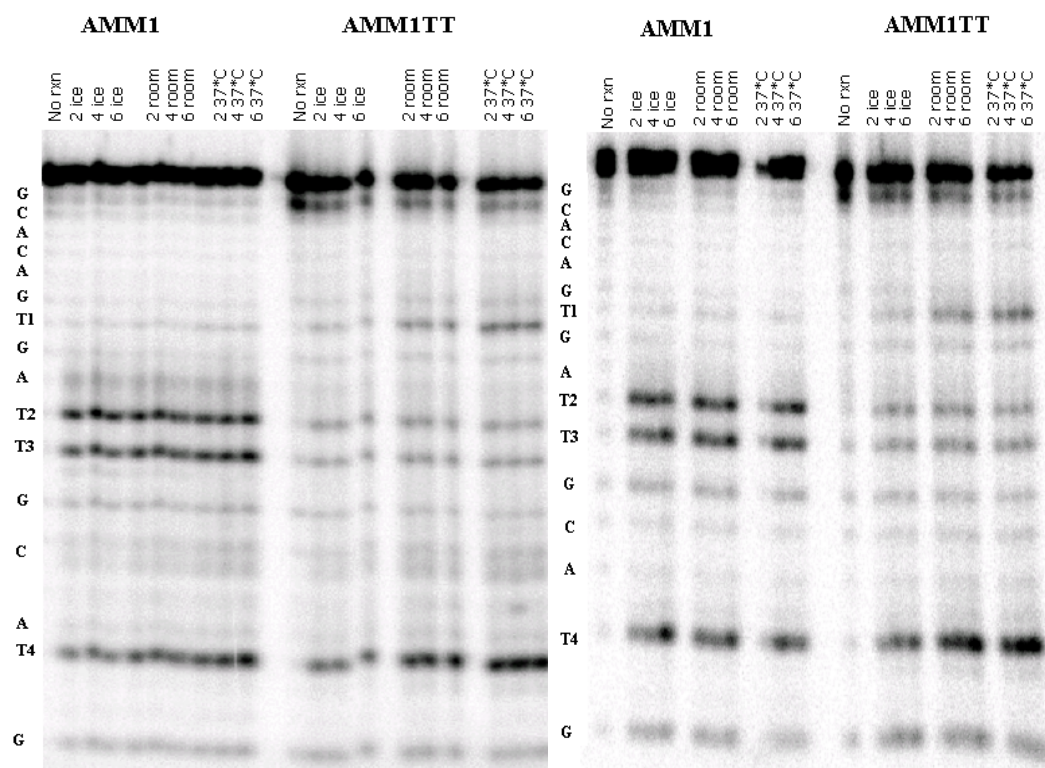
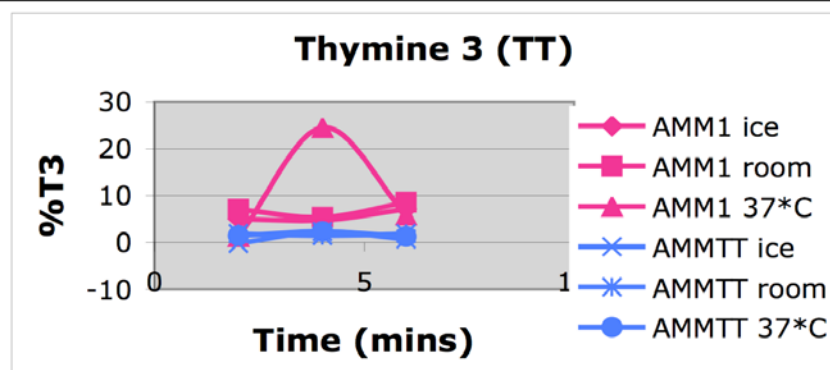
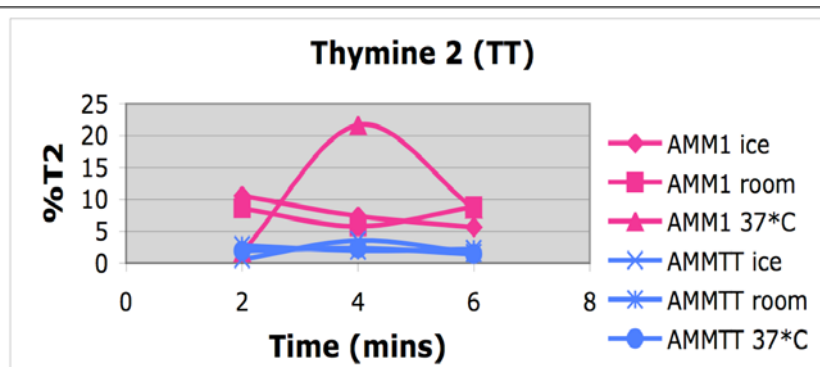
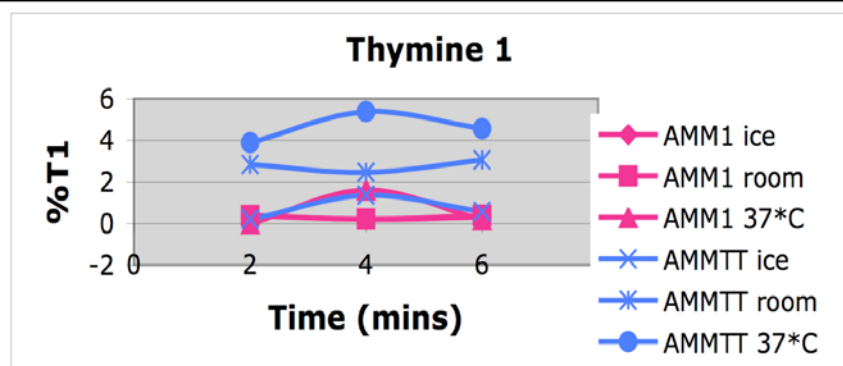


Figure 3.5. These two KMnO_4 gels show a large reactivity for the thymines around the thymine dimer in the AMM1TT*-AMM2 strand and less reactivity for the adjacent thymines in the strand AMM1*-AMM2.



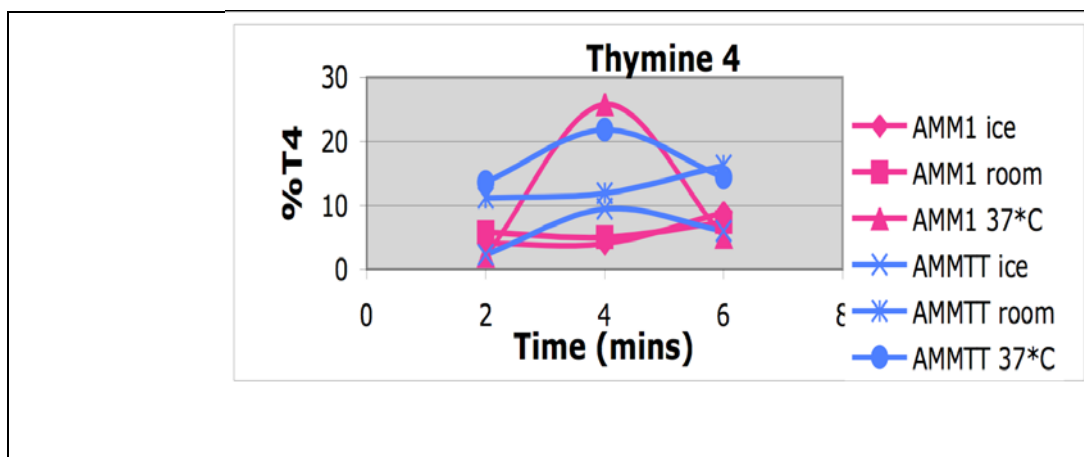


Figure 3.6. These graphs depict 4 thymines and the % reactivity at different times and on different strands. There is an obvious separation in % reactivity for all 4 of the thymines. Thymines 1 and 4 show different trends than those inside the thymine dimer (2 and 4). The information for these graphs came from KMnO_4 gel B (Figure 3.5).

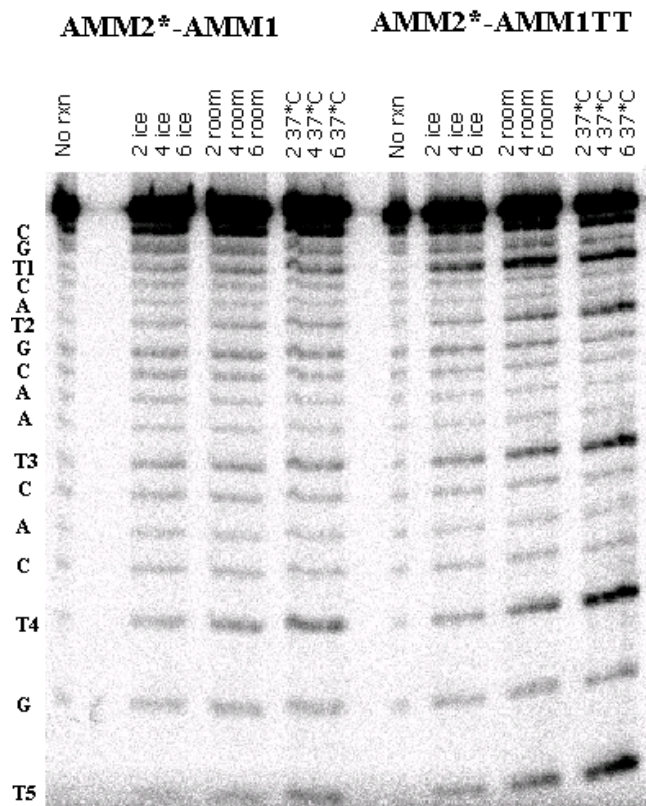
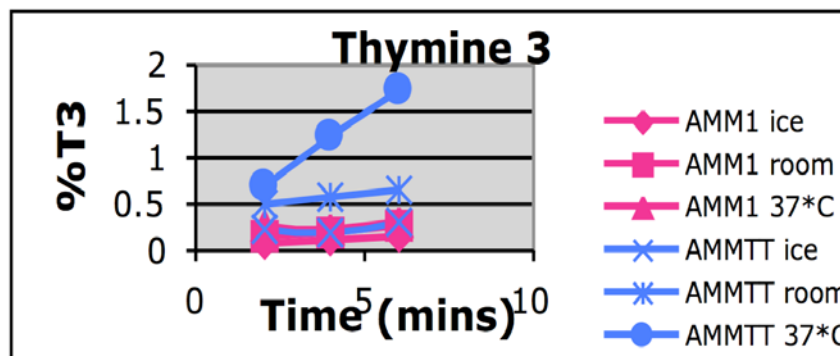
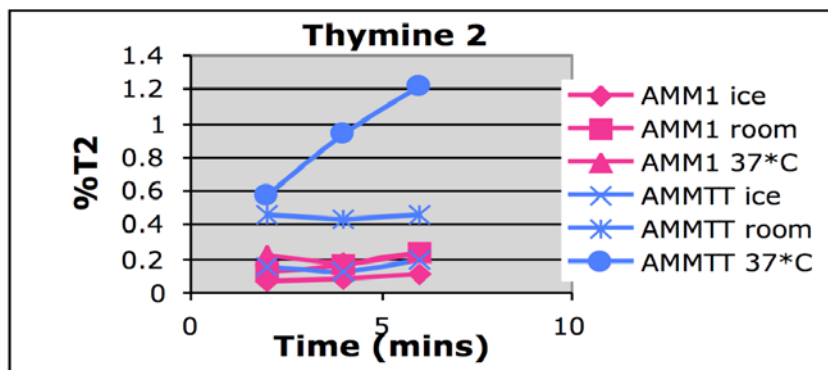
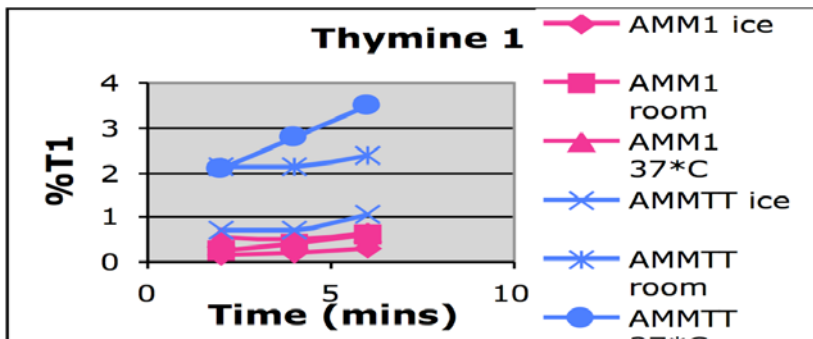


Figure 3.10. This KMnO_4 gel shows little reactivity of thymines when AMM2* is paired with AMM1 but a huge amount of reactivity when paired with AMM1TT. There are 5 thymines shown on the gel, however, only 4 were used in graphs.



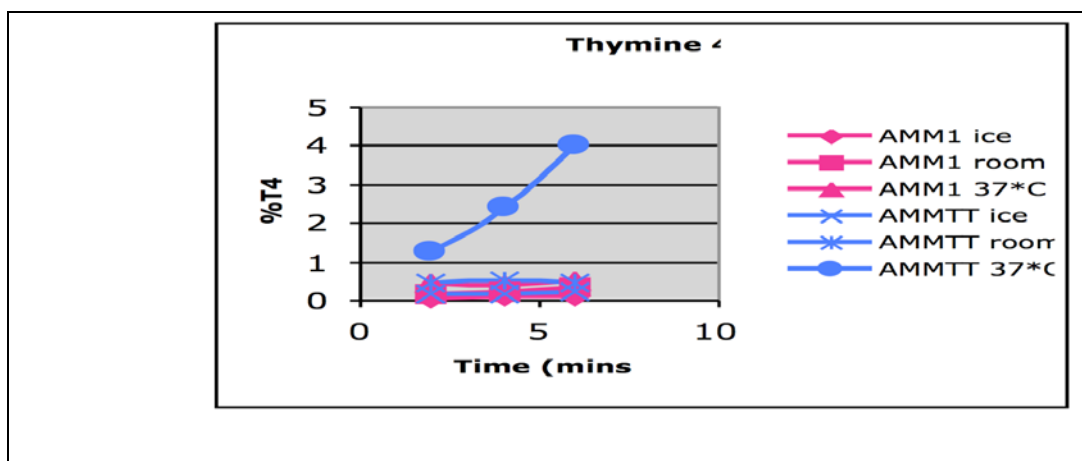


Figure 3.11. These KMnO_4 graphs show a consistently higher % of reactivity for the thymines that are cross-strand from the dimer lesion. Those thymines that are cross-strand from AMM1 show significantly less reactivity.

3.6 Diethylpyrocarbonate (DEPC) base modifying reactions:

Diethyl Pyrocarbonate reacted with the N7 of purine bases. Reactivity observed on the gel is shown in figure 3.12. The reactions on this gel were incubated at 25 °C during the reaction for multiple times. There is an increase in darkness of bands representing purine bases with increasing time. The adenine and guanine bands are more intense when the thymine dimer exists in the duplex DNA. The level of reactivity increases with time. Reactions and gels have not yet been performed to observe reactivity on the complimentary strand in the duplex.

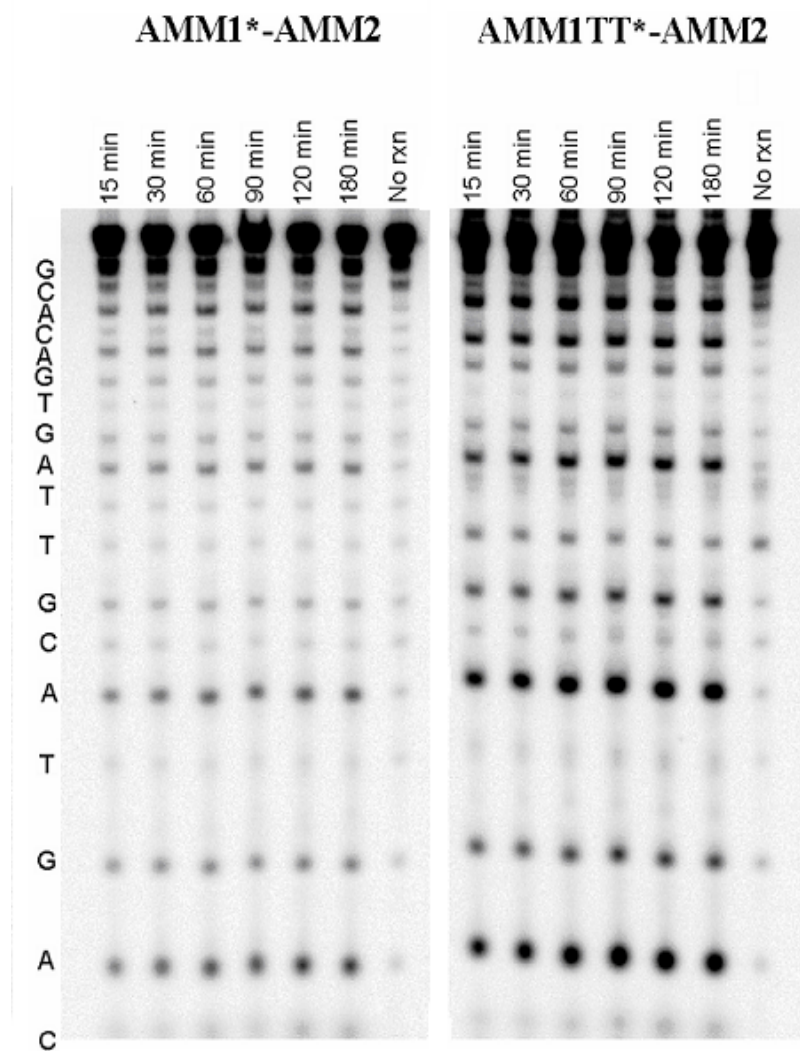


Figure 3.12. This DEPC gel shows reactivity in the duplex containing the thymine dimer at times varying from 15-180 minutes. In all lanes, DEPC was reacted with the duplex DNA at 25 °C.

3.7 van't Hoff analysis:

The results of the UV/visible spectrophotometry reveal a sigmoidal shaped graph. The graph shows a general trend of low absorbance at low temperatures, a steep increase in absorbance between 62 °C and 69 °C depending on the concentration of the duplex, and a leveling off at a higher absorbance at high temperatures. Upon taking the first derivative of the original melting curve, a second graph is developed. This graph depicts one large peak representing the T_m of the duplex. The T_m depends on the concentration of the AMM1-AMM2 duplex. Three melting curve graphs, first derivative graphs, and T_m data points were taken for each concentration and then averaged together.

The change in concentration greatly affected the melting temperature of the AMM1-AMM2 duplex. As a general trend, an increase in concentration increased the melting temperature by about 1 °C. As shown in figure 3.13, the overall absorbance for the melting curve was between 0.5 and 0.7. The average T_m for the concentration of 21.00 μM was 68.3 °C. Figure 3.17 depicts the sigmoidal melting curve of an 11.00 μM sample. The graph was between an absorbance of 0.5 and 0.7 and the average T_m at a concentration of 11.00 μM was 67.3 °C. Figure 3.18 represents a concentration of 4.2 μM . The melting curve is located between absorbencies of 0.48 and 0.6. The average T_m was 64.7 °C. Figure 3.19 shows a melting curve between the absorbance of 0.5 and 0.65 and has an average T_m of 63.7 °C at a concentration of 2 μM . Lastly, in Figure 3.20, the absorbance for the melting curve was between 0.23 and 0.28 for a

concentration of $0.79 \mu\text{M}$. The average T_m was 62.7°C . As the concentration decreases, the melting curve graph covers less of a spread of absorbencies. In addition, the melting temperature changes with concentration. The T_m decreases as concentration decreases as demonstrated by the average T_m from the first derivative graph of each concentration.

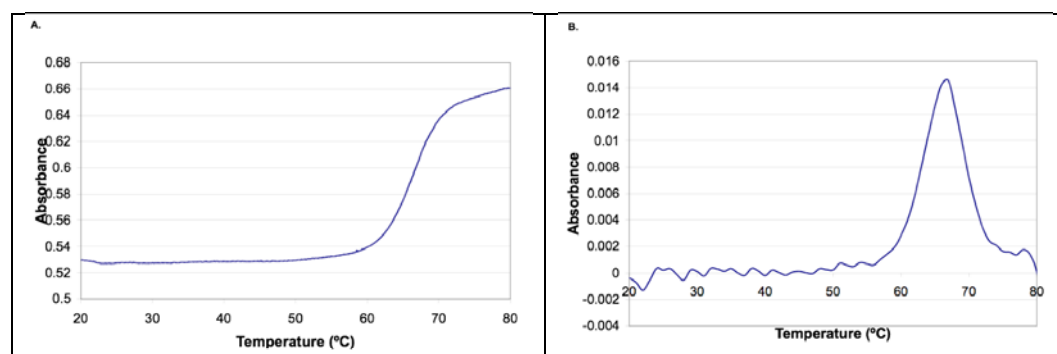


Figure 3.13. (A) Thermal melting profile of 21 μM sample of duplex AMM1/AMM2. (B) First derivative of the melting profile in panel A peaks at a T_m of 67 $^{\circ}\text{C}$.

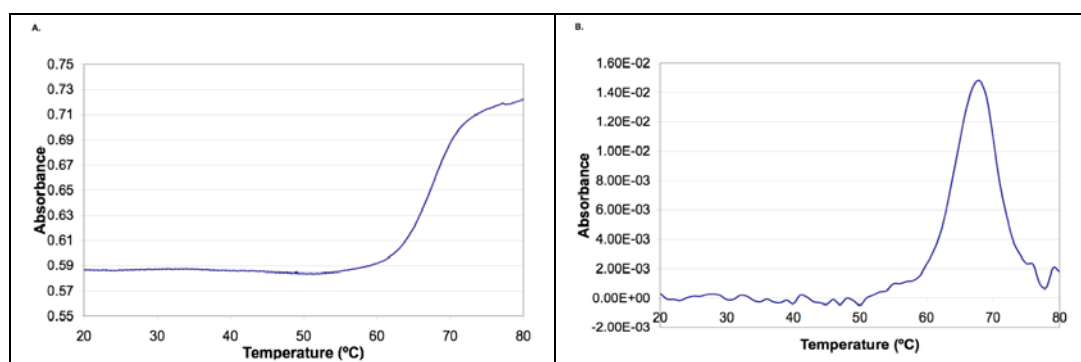


Figure 3.14. (A) Thermal melting profile of 11 μM sample of duplex AMM1/AMM2. (B) First derivative of the melting profile in panel A peaks at a T_m of 68 $^{\circ}\text{C}$.

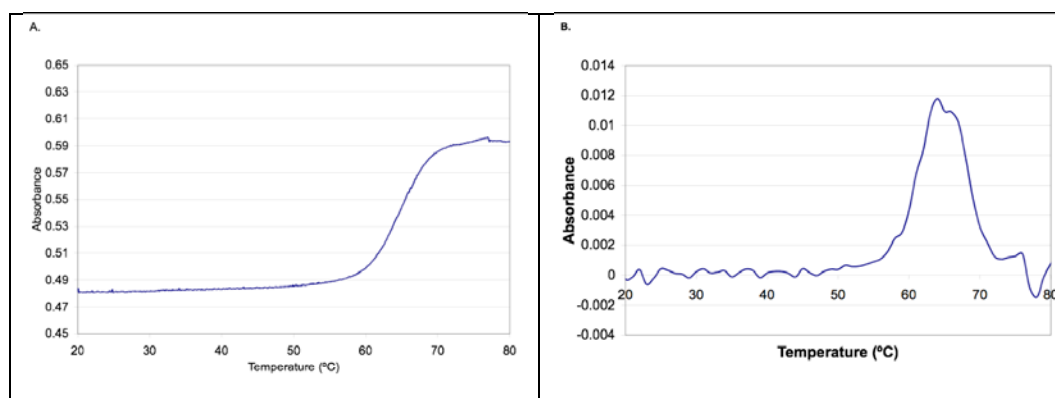


Figure 3.15. (A) Thermal melting profile of 4.2 μM sample of duplex AMM1/AMM2. (B) First derivative of the melting profile in panel A peaks at a T_m of 64 °C.

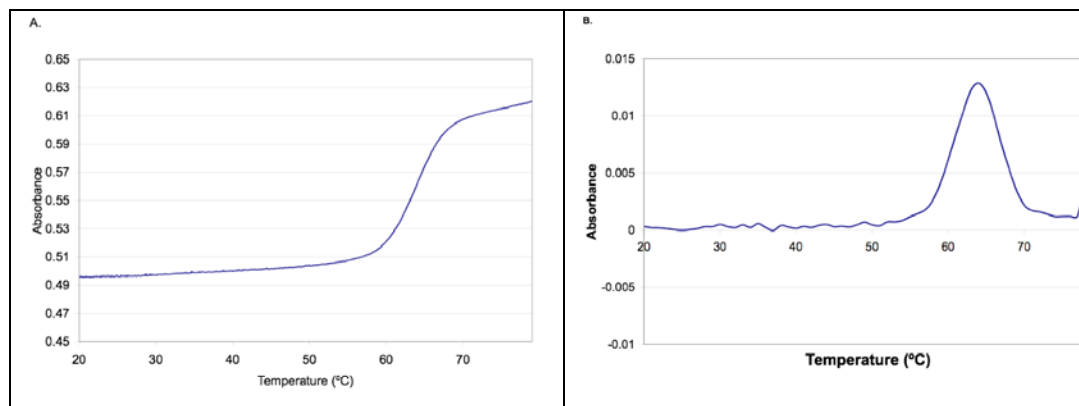


Figure 3.16. (A) Thermal melting profile of 2 μM sample of duplex AMM1/AMM2. (B) First derivative of the melting profile in panel A peaks at a T_m of 64 °C.

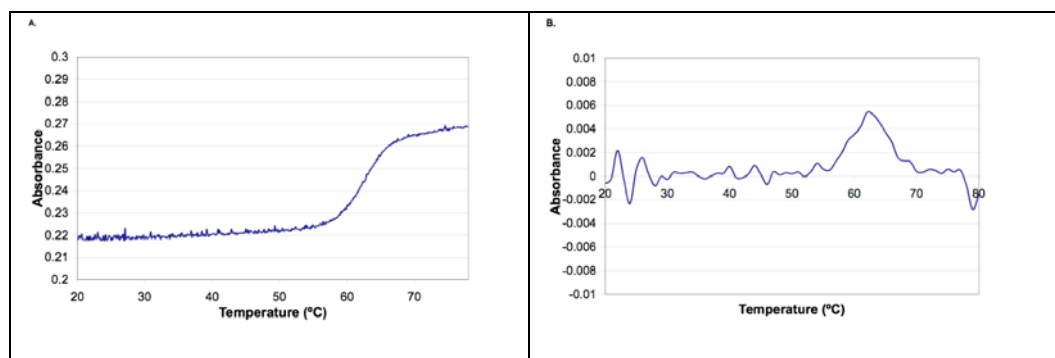


Figure 3.17. (A) Thermal melting profile of 0.79 μM sample of duplex AMM1/AMM2. (B) First derivative of the melting profile in panel A peaks at a T_m of 62 $^{\circ}\text{C}$.

3.8 van't Hoff analysis in small chemical probe buffer:

The small chemical probe reactions were run in a different buffer than the thermodynamic experiments. The thermodynamic experiments are run in 0.1 M phosphate buffer while the reactions are run in a DMS buffer system as described in the methods. In order to confirm the expected results one 11.00 μM sample was made up in DMS buffer. The results were similar for both the phosphate buffer and the DMS buffer. The first derivative graph is also shown in Figure 3.18 and 3.19.

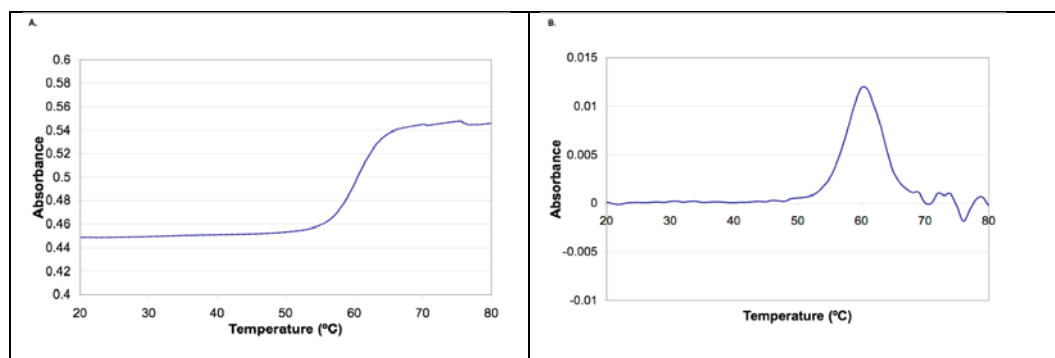


Figure 3.18. (A) Thermal melting profile of 11 μM sample of duplex AMM1/AMM2 in buffer used for DMS chemical probe experiments. (B) First derivative of the melting profile in panel A peaks at a T_m of 60 $^{\circ}\text{C}$.

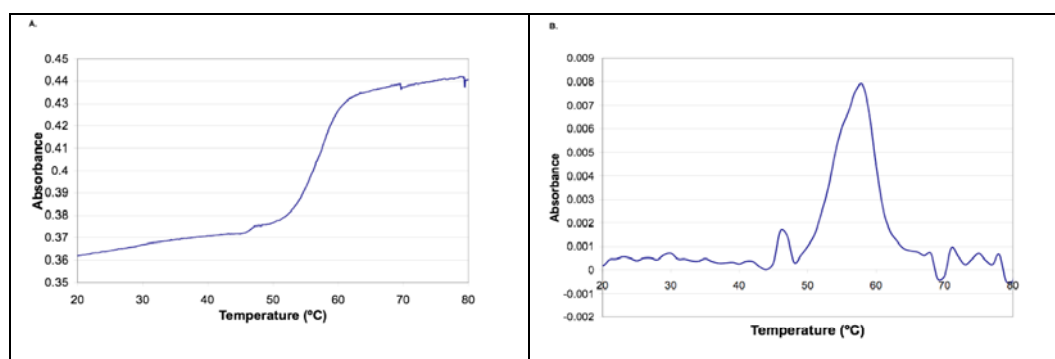


Figure 3.19. (A) Thermal melting profile of 11 μM sample of duplex AMM1/AMM2 in buffer used for DMS chemical probe experiments. (B) First derivative of the melting profile in panel A peaks at a T_m of 58 $^{\circ}\text{C}$.

3.9 First derivative graphs

In order to observe the trend of increasing melting temperatures with increasing concentrations, the overlap T_m peaks help to visualize the pattern. The overlap of first derivative graphs of the melting curves is shown in figure 3.20. The T_m peaks are distinguished by color in order to observe the visible correlation between concentration and melting temperature.

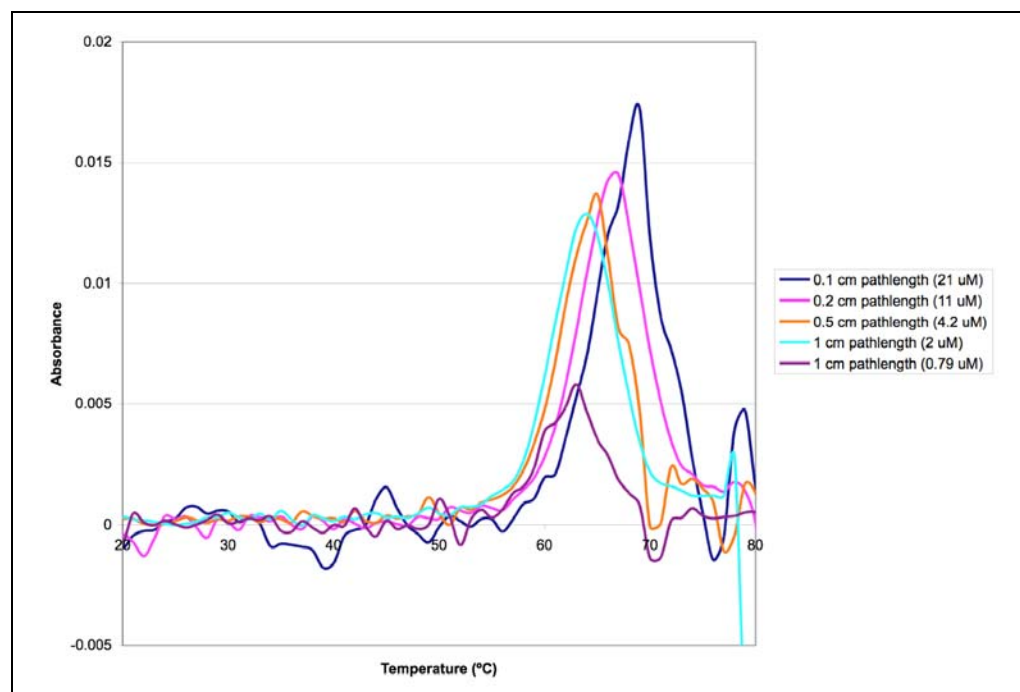


Figure 3.20. The resulting first derivative graphs of the thermal melting profiles of each concentration were plotted together to observe the correlation between T_m and concentration. Melting temperatures were extracted from each graph and used to plot a van't Hoff plot.

One problematic situation that occurs with thermal experiments is the degradation of the experimental material. In order to determine if the AMM1-AMM2 duplex degraded during the scan, a down scan was completed in addition to the up scan. The up scan is the increase in temperature from 10 °C to 90 °C. When the up scan was completed another run then went from 90 °C to 10 °C. The up scan and down scan overlapped almost exactly (refer to figure 3.21).

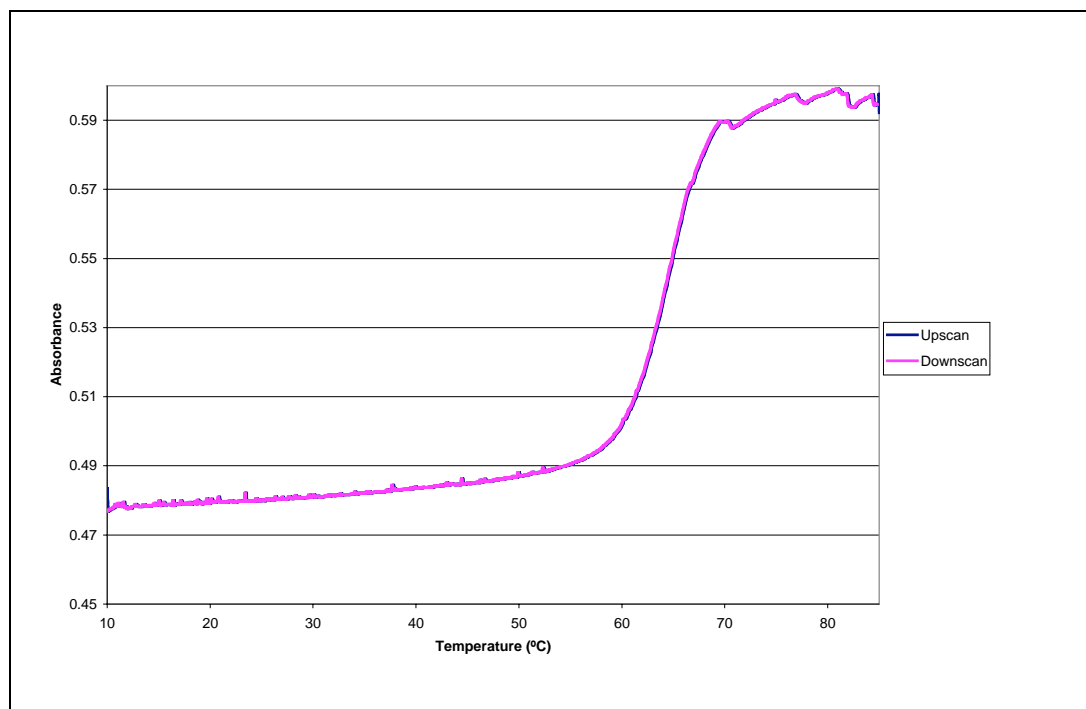


Figure 3.21. A down scan and up scan was performed at 4.2 μM to check for degradation of the oligonucleotides during heating. There was no degradation observed. The up scan and down scan are identical.

3.10 van't Hoff analysis of duplex containing the thymine dimer lesion

The results of thermal melting profile experiments elucidate a decrease in melting temperature (T_m) when the thymine dimer lesion is introduced into the duplex DNA. The graph shows a general trend of low absorbance at low temperatures, a steep increase in absorbance between 60 °C and 66 °C depending on the concentration of the duplex, and a leveling off a high absorbance at high temperatures.

The average T_m for the concentration of 21.00 μM was 66 °C. Figure 3.23 represents a concentration of 4.2 μM . The melting curve is located between absorbencies of 0.78-0.98. The average T_m was 62 °C. Figure 3.23 shows a melting curve between the absorbance of 0.78-0.98 and has an average T_m of 61 °C at a concentration of 2 μM . As the concentration decreases, the melting curve graph covers less of a spread of absorbencies. In addition, the melting temperature changes with concentration. The T_m decreases as concentration decreases as demonstrated by the average T_m from the first derivative graph of each concentration.

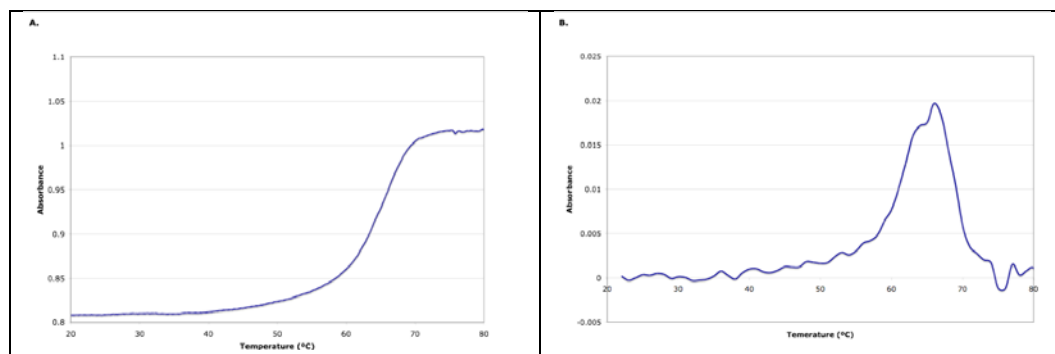


Figure 3.22. (A) Thermal melting profile of 21 μM sample of duplex AMM1TT/AMM2. (B) First derivative of the melting profile in panel A peaks at a T_m of 66 $^{\circ}\text{C}$.

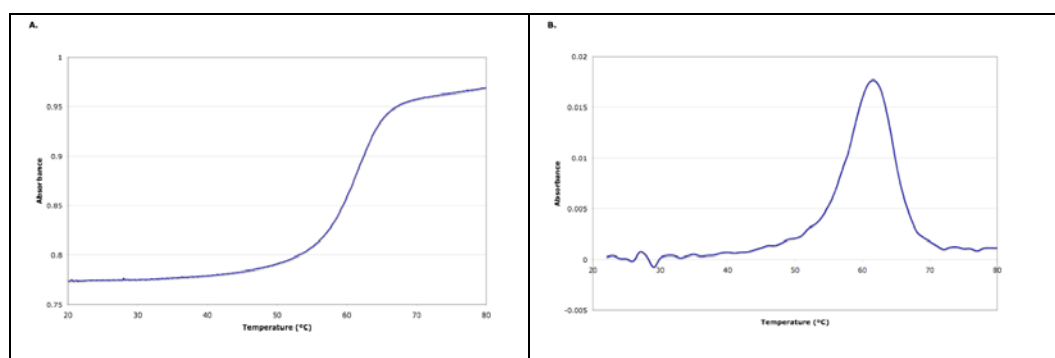


Figure 3.23. (A) Thermal melting profile of 4.2 μM sample of duplex AMM1TT/AMM2. (B) First derivative of the melting profile in panel A peaks at a T_m of 62 $^{\circ}\text{C}$.

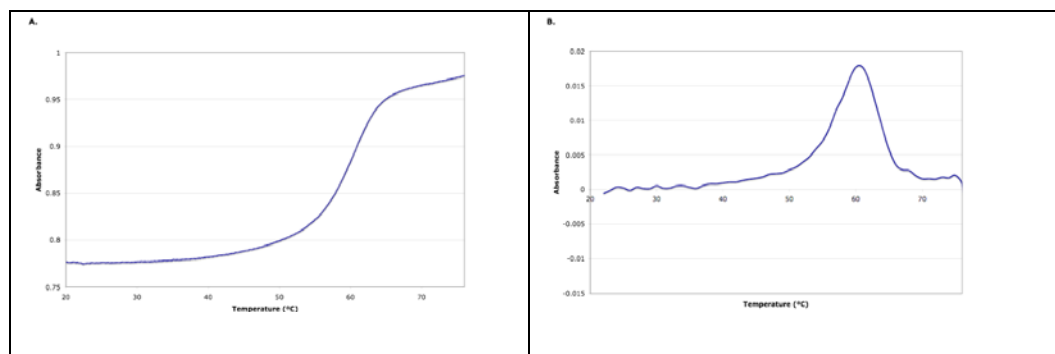


Figure 3.24. (A) Thermal melting profile of 2 μM sample of duplex AMM1TT/AMM2. (B) First derivative of the melting profile in panel A peaks at a T_m of 61 $^{\circ}\text{C}$.

Overlapping first derivative graphs depicts a gradual increase in T_m with increasing concentration. In figure, each peak represents a melting temperature. The graphs at concentrations of 2 μM , 4.2 μM , and 21 μM were plotted. The T_m points increased with concentration. The T_m s are then extrapolated from the first derivative graphs and $1/T_m$ is plotted against the natural log of the total concentration. From this data we obtain a van't Hoff plot.

Figure 3.26 is the van't Hoff plot. The result is a linear plot. From this line and an equation derived from the van't Hoff equation, we determined the ΔH , ΔG , and ΔS . These thermodynamic values are given in Figure 3.26's corresponding table.

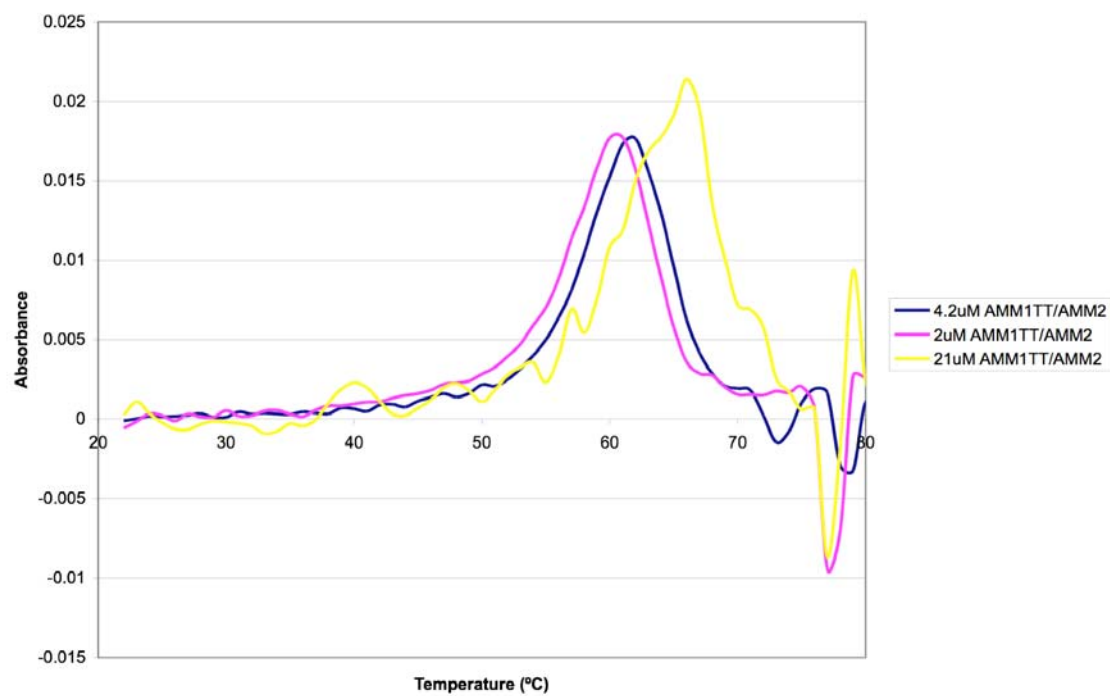


Figure 3.25. A comparison of first derivative graphs of melting profiles shows a correlation between concentration and melting temperature.

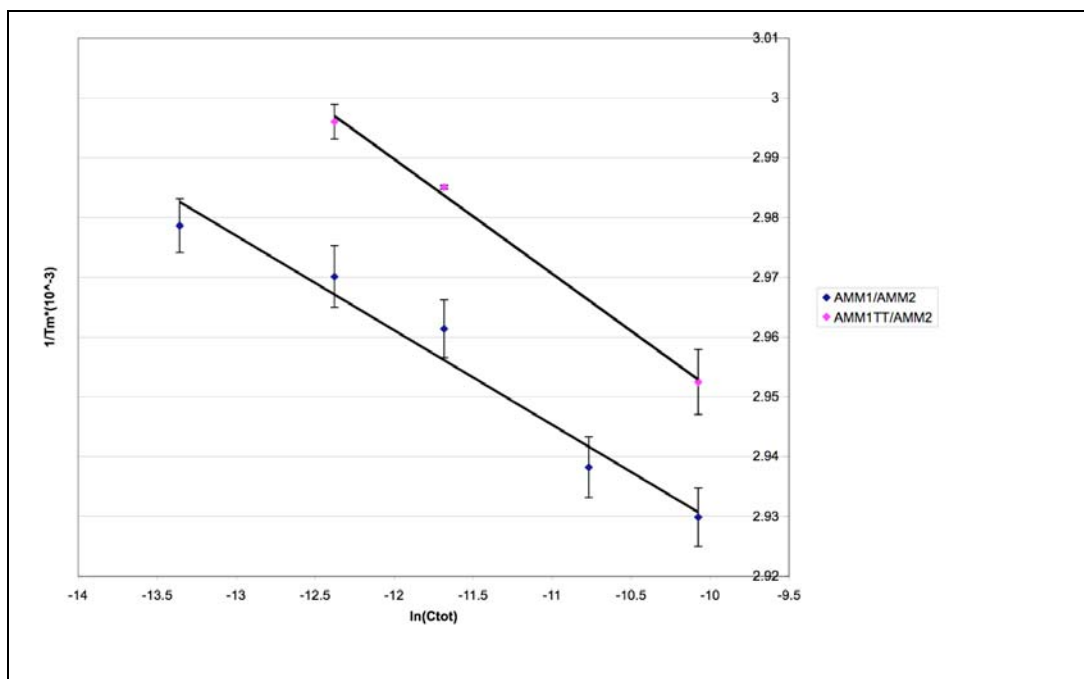


Figure 3.26. The graph depicts the linear relationship between $1/T_m$ plotted against the natural log of the total concentration. We expect the line from the AMM1-AMM2 control duplex should be lower or higher than that of the AMM1TT-AMM2 duplex. Table 3.2 presents the values for enthalpy, entropy, and free energy throughout the melting of the AMM1-AMM2 duplex.

Table 3.2. Thermodynamic data details the differences between the lesion duplex and control duplex. The results were calculated using the van't Hoff equation.

duplex	T_m , °C	T_m , °C	ΔH° kcal/mol	ΔH° kcal/mol	ΔS° cal/mol K	ΔS° cal/mol K	ΔG° at 25°C, kcal/mol	ΔG° at 25°C, kcal/mol
duplex	cal [§]	vH [†]	cal	vH	cal	vH	cal	vH
1-2	70.5 ± 0.2	68.3 ± 0.6	-131±3	-126 ±10	-363±7	-347 ± 28	-23.2 ± 2.3	-22.2 ± 2.6
1TT-2	67.4	65.7 ± 0.6	-127	-104 ± 7	-342	-285 ± 18	-25	-18.8 ± 1.7
Diff. due to T<>T	$\Delta T_m = -3.1$	$\Delta T_m = -2.6 \pm 0.8$	$\Delta \Delta H = +4$	$\Delta \Delta H = +22 \pm 12$	$\Delta \Delta S = +21$	$\Delta \Delta S = +62 \pm 33$	$\Delta \Delta G = -1.8$	$\Delta \Delta G = 3.4 \pm 3$

[§] = 40 μ M duplex, 100 mM sodium phosphate pH 7.4

[†] = 21 μ M duplex, 100 mM sodium phosphate pH 7.4. Numbers for dimer duplex samples represent only a single DSC experiment, and as such currently have no error bars.

The AMM1-AMM2 control strand may be used as a basis for comparison when comparing a duplex with the same order of bases with a thymine dimer lesion. Figure 3.27 depicts the difference between the AMM1-AMM2 control duplex and AMM1TT-AMM2 strand containing the thymine dimer. The AMM1-AMM2 (blue line) has a sigmoidal shape and higher T_m . The AMM1TT-AMM2 (pink line) has a stretched sigmoidal shape with a lower T_m . This difference will also be reflected in the enthalpy, entropy, and free energy calculations.

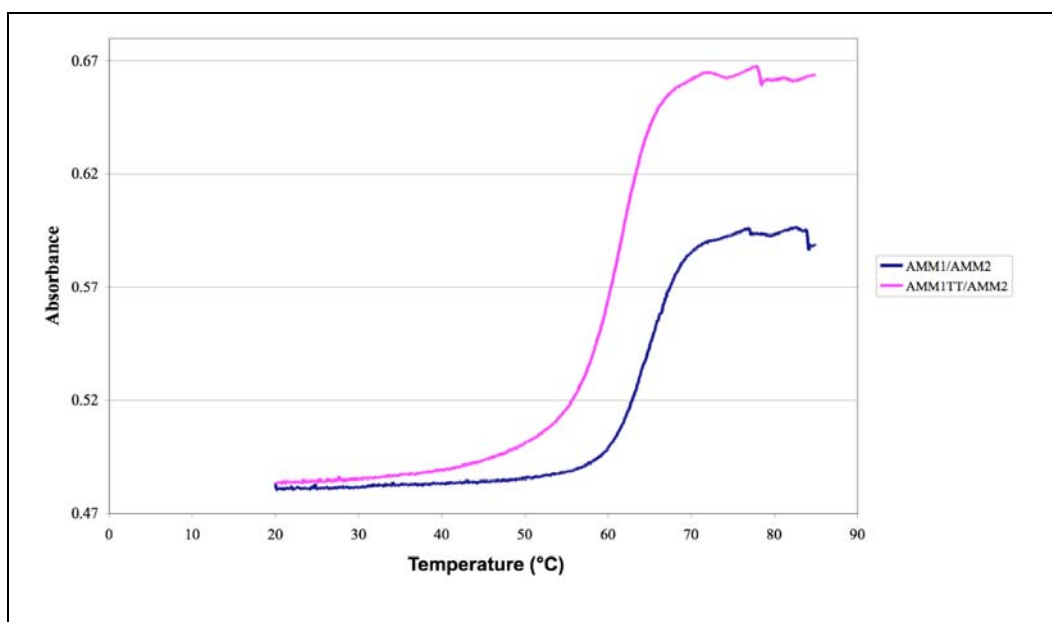


Figure 3.27. This graph depicts the shift in T_m and change in the melting graph shape between the AMM1TT-AMM2 and control AMM1-AMM2 duplex.

3.11 Differential Scanning Calorimetry:

The results of the DSC experiments show a peak at the T_m . From the peak in Figure 3.28, the graph can be normalized to obtain a value for the enthalpy, T_m , and change in heat capacity. From this information, the entropy can be determined.

Figure 3.29 displays the change in free energy that occurs as the AMM1-AMM2 duplex becomes unannealed. As the strands become separate and the temperature increases, there is a constant decrease in free energy. This decrease in free energy is due to the loss of energy as the strands separate.

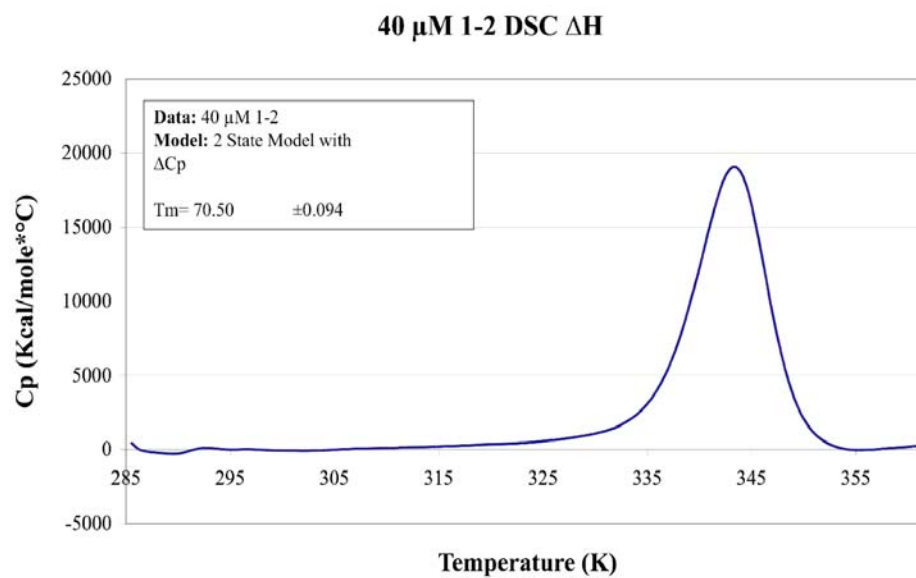


Figure 3.28. The DSC graph of the AMM1-AMM2 duplex and the values of the T_m , enthalpy, and change in heat capacity.

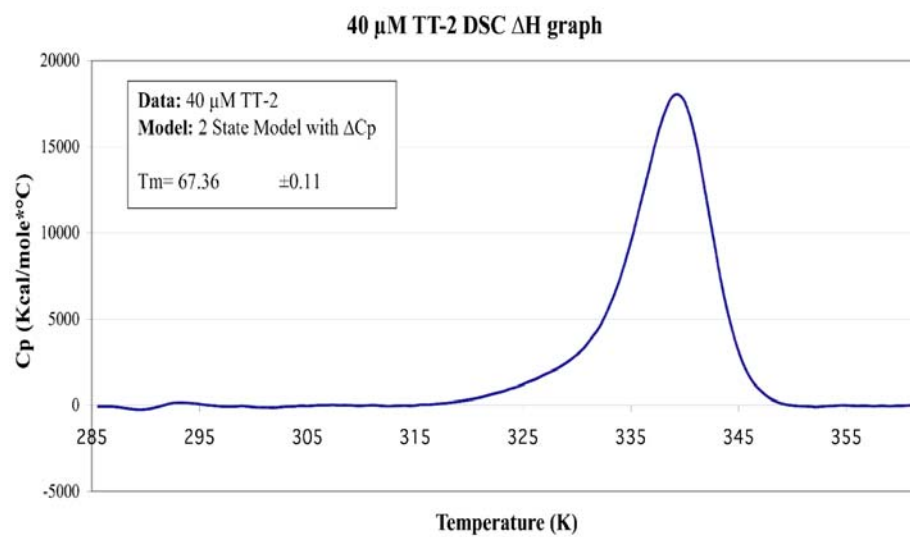


Figure 3.29. The DSC graph of the AMM1TT-AMM2 duplex and the values of the T_m , enthalpy, and change in heat capacity.

CHAPTER 4: DISCUSSION

4.1 Characterization and purification of oligonucleotides:

Oligonucleotides AMM1, AMM2, and AMM1TT were characterized using High Performance Liquid Chromatography (HPLC). Shape, size, and elution time of a peak were characteristics that allowed us to recognize the oligonucleotides and isolate them as they eluted off the column. As shown in (figure 3.2), the AMM1TT oligonucleotide took on a slightly square and broad peak. It eluted immediately before AMM1 at 18.0 minutes and was a much smaller peak. AMM1 eluted in a large, sharp peak around 21.3 minutes. AMM2 eluted similarly to AMM1 but was isolated separately from AMM1 and AMM1TT.

The cycloreversal of AMM1TT to AMM1 was successful as shown in (figure 3.1). The thymine dimer lesion was converted to separate thymines under irradiation of UV-light. This unmodified conformation was confirmed using HPLC. The ratio of AMM1TT in comparison to AMM1 decreases in the HPLC graph after cycloreversal. The AMM1TT peak that elutes at 18.0 minutes decreases in comparison to the AMM1 peak that elutes at 21.3 minutes only after cycloreversal of the thymine dimer. This indicates that our synthesis did, in fact, result in the formation of the thymine dimer lesion.

4.2 Accessibility to Small Chemical Probes:

It has been shown that the thymine dimer lesion significantly perturbs duplex DNA through thermodynamic and structural studies. Structurally, adenines cannot bind to the thymine dimer. This causes a kink in the DNA. The thymine dimer lesion perturbs the DNA by bending the double helix up to 30°. This perturbation has been shown to thermodynamically destabilize the duplex DNA. We investigate the reactivity of bases localized around or down-strand from the thymine dimer lesion. The observed increase in reactivity in the presence of the thymine dimer is shown through base modifying chemical probes.

The results acquired from this experiment reflect the thymine dimer lesion's effect on the structure of DNA and ultimately, on the reactivity of the bases adjacent to the thymine dimer lesion. The thymine dimer bends the B-form DNA at an angle of up to 30 °C. This bending may cause bases around the dimer to be more reactive to base modifying chemical probes. To test this, DMS, KMnO_4 , and diethylpyrocarbonate (DEPC) were reacted with duplex DNA. The two strands used in the reactions were AMM1* -AMM2 and AMMTT* -AMM2.

The results of the reactions with Dimethyl Sulfate (DMS) show similar reactivity of guanines between AMM1*-AMM2 and AMMTT*-AMM2. DMS methylates the N7 of guanine. The results show that each guanine has an N7 that is accessible to methylation by DMS. For guanines 1-4 there is an obvious overlap of reactivity whether the guanine is located in the AMM1*-AMM2 strand or the AMMTT*-AMM2 strand. It is likely that these results are due to the fact

that N7 of guanine is located in the major groove of the DNA. It is accessible to DMS with or without the existence of the thymine dimer lesion in the DNA duplexes.

The DMS reactions for strands AMM2*-AMM1 and AMM2*-AMM1TT showed similar results to the radioactive AMM1 and AMM1TT strands. In most cases, the data from the DMS gels overlapped. This shows that the guanines were accessible to DMS on the complimentary strand as well. Both the control and the experimental strand showed results with overlapping reactivity. The existence of the thymine dimer lesion had little effect on the reactivity of the guanines and accessibility of guanines to DMS is the same for those in the control strand and those in the experimental strand.

The results of the KMnO_4 reaction of strands AMM1*-AMM2 and AMM1TT*-AMM2 are complex and interesting. Thymines 1 and 4 are three bp and 4 bp away from the thymine dimer lesion, respectively. Despite the distance from the thymine dimer, these bases are more reactive in DNA duplex AMM1TT*-AMM2. The bases are more accessible because of the bending of the DNA. The KMnO_4 solution is also able to access the C5, C6 double bond in adjacent thymines. Thymines 1 and 4 on the control strand, AMM1*-AMM2 were not as reactive as those in the dimer duplex. While the C5, C6 bond is available for the KMnO_4 reaction, the duplex is more stable without the thymine dimer lesion.

Thymines 2 and 3 were part of the thymine dimer or neighboring thymines on the control strand. There was minimal reactivity of the dimer in the AMM1TT*-AMM2 strand. The dimer is not reactive with KMnO_4 as a base modifier because the thymine dimer has undergone cycloaddition at the C5, C6 double bond. Neighboring thymines 2 and 3 on the AMM1*-AMM2 control strand, however, showed great reactivity at this location. The reactions at this site occur here because the C5, C6 double bond in thymines 2 and 3 was accessible to the KMnO_4 solution.

Looking at DNA strands AMM1*-AMM2 and AMM1TT*-AMM2 we were able to see an increased reactivity with the bases around the thymine dimer supporting the hypothesis that the thymine dimer has a large disturbing effect on DNA in its vicinity. In the DMS reaction all guanines were accessible to DMS and all of them reacted equally in the dimer as in the control duplex. Also, the thymines within the thymine dimer lesion duplex were not accessible to the KMnO_4 .

In the KMnO_4 reactions, some samples were overcleaved and ran through the gel so that the tops of the wells were left with little radioactivity. This overcleavage gives high percentage of reactivity on the graphs. They are outliers on the plots. When overcleavage occurs, only the 5' fragment retains the $\gamma^{32}\text{P}$ label making it the only fragment visible on the gels. To understand this data, one must observe overall trends in the curves rather than the individual data points.

The KMnO_4 reaction on the complementary strand supported the interesting results on the AMM1*/AMM1TT strand. Because thymines in AMM2*-AMM1 were not destabilized by perturbation induced by the thymine dimer, cross-strand thymines showed minimal reactivity. The cross-strand thymines in the AMM2*-AMM1TT duplex, however, were clearly more reactive. Accessibility to KMnO_4 does not seem to be a factor at play at the site of the thymine. All of the thymines are normal with accessible C5, C6 double bonds. Therefore, the factor causing these huge amounts of reactivity on the AMM1TT-AMM2* strand must be due to the existence of the thymine dimer lesion. These experiments with the complementary strand also showed much less overcleavage and were more reliable.

Diethylpyrocarbonate (DEPC) modifies the N7 position of purine bases. As shown in figure (3.12), guanine and adenine bases were highly reactive with DEPC when in the presence of the thymine dimer lesion. This reactivity was not visible in the duplex without the lesion. At 25 °C, there was a consistently high amount of reactivity of guanine and adenine bases in the presence of the thymine dimer.

4.3 Thermodynamic Experiments:

Spectroscopic and calorimetric techniques were used to assess the thermal stability of the unmodified duplex in comparison with the modified duplex. From the calculated thermodynamic parameters, the presence of the lesion causes a visible increase in entropy and decrease in enthalpy. Therefore, the thymine dimer lesion is entropically stabilizing and enthalpically destabilizing. This trend has been observed with other lesions including cisplatin adducts, the 3, N4-deoxyethenocytosine (εC) exocyclic adduct, and 8-oxoguanine as described earlier.

Thermodynamic parameters depend on concentration of the duplex. The thermal stability of a duplex increases as a function of concentration. Raising the concentration from 0.79 μM to 21 μM caused the T_m to increase. This is consistent for both the modified and unmodified duplexes.

The melting profiles of the upscan (heating) and downscan (cooling) show that denaturation and renaturation of the unmodified duplex is completely reversible. With a temperature range of 20-90 °C and heating and cooling rates of 0.2 °C/minute, the melting profiles for the unmodified duplex were nearly identical (Figure 3.21). This property of reversibility in unmodified DNA has been observed with the cisplatin lesion. The study observes a non-reversible model for duplex DNA modified with the cisplatin lesion. It is likely a similar trend will be observed when denaturation and renaturation of the thymine dimer lesion duplex is carried out if the DNA does not become damaged as a result of

heat. Poklar *et al.* suggests that the non-reversible model may be caused by a kinetic constraint such as a metastable state. This limitation must be considered so as not to confuse a kinetically trapped state with equilibrium (Poklar *et al.*, 1996).

The modified duplex DNA had a lower melting temperature (T_m) in comparison to the unmodified duplex. The T_m shifted from the unmodified duplex to the duplex containing the thymine dimer lesion depending on concentration. This suggests that the thymine dimer lesion thermally destabilized the duplex. This destabilization may be due to perturbations in the DNA such as base unstacking.

In order to obtain thermodynamic parameters using spectroscopy, the T_m of each concentration was extracted from the melting profiles and averaged. The T_m and concentration were then used in a van't Hoff analysis. A plot of the reciprocal of the T_m and the natural log of the concentration reveal the shift in T_m between AMM1 and AMM1TT. This model assumes that the relationship between concentration and T_m is linear and plots the data as such. The y-intercept and slope of the lines were plugged into the van't Hoff equation to determine enthalpy and entropy (Eq. 1). The shift between the modified and unmodified DNA is visible in the van't Hoff plot.

The van't Hoff analysis assumes a two state model. Therefore, it describes a DNA molecule without intermediate states that might influence the thermodynamics. A two-state model predicts a molecule that remains completely

annealed (double-strand) at lower temperatures, becomes completely unannealed (single-strand) at high temperatures, and is 50% single-strand and 50% double-strand at the T_m . This model is assessed using obtained data.

The calculated results of the van't Hoff analysis gave very small enthalpy for the modified DNA in comparison to the unmodified DNA. On the other hand, the entropy for the modified DNA was very high and much lower for the unmodified DNA. These changes are understandable because a lesion would inflict disorder on a DNA duplex. This is visible in the increase in entropy. The enthalpy on the other hand would decrease because the thymine dimer cannot bind with adenine bases. Enthalpy is directly related to the bonds in the center of the DNA helix. The missing hydrogen bonds to adenine would cause a reduction in enthalpy.

Differential Scanning Calorimetry was used to confirm these values. As shown in table 2, DSC data is very similar to that obtained through the van't Hoff analysis. It is interesting that the slope as ΔC_p increases has a different shape from the decreasing slope. This may suggest that using a two state model such as the van't Hoff analysis or 2-state DSC model is not the best way to analyze the data. There may be an intermediate state contributing to thermodynamic parameters.

4.4 Chemical probe and thermodynamic experiments relate to previous studies:

The DNA duplex containing a thymine dimer lesion has often been depicted using structural studies such as X-ray crystallography and NMR. One study depicts DNA containing the thymine dimer to bend 30 ° toward the major groove and an area of about 9° of unwinding (Park *et al.*, 2002).

We speculate that the thymine dimer lesion may affect the way the DNA moves normally as a static molecule. Within it's environment, duplex DNA is not static. It undergoes stretching and base flipping naturally. We think that the thymine dimer lesion causes destabilization to the duplex causing an increase in base flipping. It is this increased base flipping that exposes the bases surrounding the lesion to the environment making them more accessible to conditions outside the DNA helix.

4.5 Considering kinetic base modification in addition to thermodynamic and structural studies will provide a better understanding of destabilization

The two common procedures for understanding the consequence of DNA lesions include the thermodynamic studies and a structural approach. Structural studies such as X-ray crystallography display a static molecule. Utilizing a 2-state calorimetric model and van't Hoff equation assumes that DNA melts in only two steps at high temperature conditions. These assumptions may not fit all models of lesion-induced destabilization.

Structural studies such as X-ray crystallography are used to obtain a structure for duplexes containing lesions. These structures are displayed as a static molecule and are helpful in understanding perturbation and degrees of bending. However, biologically relevant molecules are not static. They vibrate and move within their environment. DNA as a static molecule may experience bases randomly flipping out of the helix and quickly returning to position inside of the helix due to hydrophobic interactions. It is possible that a destabilizing lesion causes the bases to flip out of position more often. We see this in the base modifying experiments. We believe the increased reactivity is due to bases flipping out of the helix and being modified. Therefore, using kinetic experiments to compliment structural analysis is important.

We question whether it is acceptable to assume a two-state model when calculating the thermodynamic parameters for the melting of the oligonucleotide containing the thymine dimer lesion. In both calorimetric and spectroscopic

methods, the shape of melting profile is different for modified and unmodified duplexes. Just as melting began to occur, there was a visible difference in slope. This suggests that the duplex containing the thymine dimer could have been melting in more than two states. Perhaps a two-state model was not appropriate for studying and calculating the thermodynamic parameter changes of a duplex containing the thymine dimer lesion.

Thermodynamic experiments are executed by raising temperature conditions from biologically relevant temperatures to high temperatures. Changes in thermal and enthalpic stability are usually calculated at high temperatures. However, the context of this experiment occurs at much lower temperatures. Base Excision Repair enzymes must recognize the lesion under biological conditions. Kinetic experiments using chemical modifying probes show reactivity at 37 °C, 25 °C, and sometimes 0 °C. For this reason it is important to consider both kinetic and thermodynamic destabilization.

4.6 Future Studies:

Studying other lesions and their effect on duplex destabilization is of interest. Smaller lesions may have a less destabilizing effect on DNA because they do not perturb the DNA as much as the bulky thymine dimer lesion. It would be interesting to see if the size or bulkiness of the lesion plays a role in the way the DNA acts. In addition, thymine dimer lesions perturb duplex DNA because complimentary adenine bases cannot bind to the mutated thymine bases. It would be interesting to perform these experiments on lesions that continue to form bonds with bases even after mutation and then compare the results to lesions that cannot form bonds with complimentary bases, such as the thymine dimer. It would be interesting to explore this because current studies see destabilization in adducts which form from crosslinking in the duplex (Gelfand *et al.*, 1998 and Poklar *et al.*, 1996).

Another interesting study would take sequence context surrounding the lesion into account when performing thermodynamic analysis. Experiments varying sequence context in thermodynamic experiments while exploring the effects of an exocyclic adduct led to inconclusive results. In this experiment, Gelfand *et al.* found that sequence context had little effect on the destabilization induced by the adduct (Gelfand *et al.*, 1998). Variation of sequence context may affect kinetic destabilization as well. A higher number of GC pairs may strengthen the stability of the duplex because they form three hydrogen bonds. It

would be interesting to see the results of chemical probe experiments with varying sequence context.

The next major step in this project will be to acquire NMR data on the duplex containing the thymine dimer lesion. This structural data would be complimentary to thermodynamic and kinetic data. In addition, base modifying chemical probes will be used to better understand destabilization induced by the 8-oxoguanine lesion.

REFERENCES

- 1) Breslauer, K.J., Frank, R., Blocker, H., Marky, L.A. (1986) Predicting DNA duplex stability from the base sequence. *Proc. Natl. Acad. Sci. USA*, **83**, 3746-3750.
- 2) Brown, T., Hunter, W.N., Kneale, G., Kennard, O. (1986) Molecular structure of the G:A base pair in DNA and its implications for the mechanism of transversion mutations. *Proc. Natl. Acad. Sci. USA*, **83**, 2402-2406.
- 3) Bruice, P.Y. Organic Chemistry. Prentice-Hall, Inc. 1999.
- 4) Bruner, S.D., Norman, D.P.G., Verdine, G.L. (2000) Structural basis for recognition and repair of the endogenous mutagen 8-oxoguanine in DNA. *Nature* **403**, 859-866.
- 5) Chalikian, T.V., Volker, J., Anafi, D., Breslauer, K.J. (1997) The Native and the Heat-induced Denatured states of alpha-Chymotrypsinogen A: Thermodynamic Spectroscopic Studies. *JMB*, 237-252.
- 6) Cavaluzzi, M.J. and Borer, P.N. (2004) Revised UV extinction coefficients for nucleoside-5'-monophosphates and unpaired DNA and RNA. *Nucleic Acids Research* **32**, 1-9.
- 7) Devor, E.J. and Behlke, M.A. (2005) Oligonucleotide yield, resuspension, and storage. *Integrated DNA Technologies*, 1-11.
- 8) Ehresmann, C., Baudin, F., Mougel, M., Romby, P., Ebel, J.P., Ehresmann, B. (1987) Probing the structure of RNAs in solution. *Nucleic Acids Research* **15**, 9109-9128.
- 9) Friedberg, E.C., Walker, G.C., and Siede, W. (1995) DNA repair and mutagenesis. ASM Press. Washington, D.C. 1-698.
- 10) Gelfand, C.A., Plum, G.E., Mielewczyk, S., Remeta, D.P., Breslauer, K.J. (1999) A quantitative method for evaluating the stabilities of nucleic acids. *Proc. Natl. Acad. Sci. USA*, **96**, 6113-6118.
- 11) Gelfand, C.A., Plum, G.E., Grollman, A.P., Johnson, F., Breslauer, K.J. (1998) The impact of an exocyclic cytosine adduct on DNA duplex properties: significant thermodynamic consequences despite modest lesion-induced structural alterations. *Biochemistry*, **37**, 12507-12512.

- 12) <http://www.glenres.com/index.html?/GlenReports/GR16-21.html>
- 13) <http://138.192.68.68/bio/Courses/biochem2/GeneIntro/DNAandRNAIntro.html>
- 14) <http://www.public.asu.edu/~iangould/reallife/thymine/thymine.html>
- 15) http://www.wordiq.com/knowledge/images/7/76/DNA_labels.jpg
- 16) Husain, I., Griffith, J., Sancar, A. (1988) Thymine Dimers bend DNA. *Proc. Natl. Acad. Sci. USA*, **85**, 2558-2562.
- 17) Malhowski, A. (2005) Examining Kinetic and Thermodynamic DNA destabilization Caused by the *cis-syn* Thymine Dimer Lesion Using Small Molecular Probes. Mount Holyoke College Undergraduate Honors Thesis.
- 18) Marnett, L.J. and Plataras, J.P. (2001) Endogenous DNA damage and mutation. *Trends in Genetics* **17**, 214-221.
- 19) Nelson, D. and Cox, M. Lehninger Principles of Biochemistry. Fourth Ed. W.H. Freeman and Company. New York. 2004.
- 20) Nunez, Megan. (2004) Needle in a Haystack: Removing Base Lesions from DNA. Mount Holyoke College Publication.
- 21) Park, H., Zhang, K., Ren, Y., Nadji, S., Sinha, N., Taylor, J.S., Kang, C. (2002) Crystal structure of a DNA decamer containing a *cis-syn* Thymine-dimer. *Proc. Natl. Acad. Sci. USA*, **99**, 15965.
- 22) Plum, E.G. and Breslauer, K.J. (1994) DNA lesions. A thermodynamic perspective. *Ann N Y Acad Sci.* **726**, 45-55.
- 23) Poklar, N., Pilch, D.S., Lippard, S.J., Redding, E.A., Dunham, S.U., Breslauer, K.J. (1996) Influence of cisplatin intrastrand crosslinking on the conformation, thermal stability, and energetics of a 20-mer DNA duplex. *Proc. Natl. Acad. Sci. USA*, **93**, 7606-7611.
- 24) Sambrook

